

# Distinguishability of Hyper-Entangled Bell States with Linear Devices

**Neal C. Pienti**

Theresa W. Lynn, Advisor

May, 2011

**HARVEY MUDD**  
COLLEGE

Department of Physics

Copyright © 2011 Neal C. Piseni.

The author grants Harvey Mudd College the nonexclusive right to make this work available for noncommercial, educational purposes, provided that this copyright statement appears on the reproduced materials and notice is given that the copying is by permission of the author. To disseminate otherwise or to republish requires written permission from the author.

# Abstract

Measuring the entangled Bell state of two particles is a crucial step in numerous quantum communication protocols, such as quantum teleportation and quantum dense coding. For a variety of practical reasons, it is very attractive to stipulate that the Bell state measurements be performed using devices constrained to linear evolution and local measurement. However, this constraint limits our ability to distinguish unconditionally between any two Bell states. In this thesis, I present new results bounding Bell-state distinguishability for hyper-entangled particles, that is, for two particles entangled in  $n$  qubit degrees of freedom. Specifically, I show that linear evolution, local measurement devices can at best distinguish between  $2^{n+1} - 1$  (out of  $4^n$ ) hyper-entangled Bell states. I also prove that any given measurement outcome is bounded from below in the number of states it can select from the total state space. The proofs shown in this thesis cast light on the underlying structure of Bell-state measurements using linear devices, and provide an intuitive understanding of where the bounds on distinguishability originate.



# Contents

<b>Abstract</b>	<b>iii</b>
<b>Acknowledgments</b>	<b>ix</b>
<b>1 Introduction</b>	<b>1</b>
<b>2 Entanglement and the Bell Basis</b>	<b>5</b>
2.1 Introduction . . . . .	5
2.2 Mathematical foundation . . . . .	7
2.3 The Bell Basis and Hyper-entangled states . . . . .	9
2.4 $\Phi/\Psi$ Signatures . . . . .	12
<b>3 Protocols Relying on Bell-state Discrimination</b>	<b>15</b>
3.1 Introduction . . . . .	15
3.2 Quantum Teleportation . . . . .	16
3.3 Other protocols . . . . .	20
<b>4 Setup and Previous Work</b>	<b>21</b>
4.1 Introduction . . . . .	21
4.2 Mathematical formalism . . . . .	23
4.3 Previous Work . . . . .	27
<b>5 Proof of maximal distinguishability</b>	<b>33</b>
5.1 Introduction . . . . .	33
5.2 Proof . . . . .	33
<b>6 Proof of minimum class size</b>	<b>39</b>
6.1 Introduction . . . . .	39
6.2 Relationship between Bell states and joint-particle input states	41
6.3 Proof of minimum Bell-state class size . . . . .	45

<b>7 Conclusion</b>	<b>49</b>
<b>A Alternate minimum class-size proof</b>	<b>51</b>
A.1 Notation and representations of Bell/detector states . . . . .	51
A.2 Proof of no-go theorem for general $n$ . . . . .	53
<b>Bibliography</b>	<b>61</b>

# List of Figures

1.1	<i>Breakdown of Bell-state classes.</i> A linear evolution, local measurement device can differentiate between at most three separate Bell-state classes. Here, a division of the four Bell states into different classes demonstrates how 50% of the time one will measure a state in Class 1 and hence make an ambiguous measurement. This limits the efficiency of applications such as quantum teleportation, which require an unambiguous measurement to succeed. . . . .	2
3.1	<i>Schematic of a quantum teleportation device.</i> Alice and Bob each possess one member of an EPR pair in the singlet state $ \Psi^-\rangle$ . To teleport the state of some particle $Q$ , Alice performs a Bell-state measurement between $Q$ and her half of the entangled pair. She broadcasts the result to Bob via some classical channel, who then performs one of four simple transformations given by Equations (3.10)—(3.13) on his particle to recover the original state of $Q$ . . . . .	17
4.1	<i>Schematic of a linear evolution, local measurement device.</i> A pair of particles enter the measurement apparatus via separate spatial channels (Left and Right). Each particle evolves independently of the other (linear evolution), hence the unitary evolution of single-particle input modes to the set of output modes. Local measurement registers two clicks in the detectors situated at each output mode, projecting the system into a product state of two single-particle output modes (possibly the same mode twice). . . . .	25

- 4.2 *Schematic of an optimal LELM apparatus.* Two photons entangled in variables  $1 \dots n$  are incident on a 50/50 beamsplitter, which interferes  $|\varphi_{2s-1}\rangle$  and  $|\varphi_{2s}\rangle$ . Evolution  $M_{1\dots n}$  separates particles by values of the  $n$  variables, so detection is a projective measurement in the  $\{|0\rangle, |1\rangle\}^{\otimes n}$  basis. (If the beamsplitter does not preserve variables  $1 \dots k$ ,  $M_{1\dots k}$  must precede the beamsplitter stage while  $M_{k+1\dots n}$  can follow.) For one-variable Bell states of photon polarization,  $M_{1\dots n}$  is simply  $M_1$  and can be realized with a polarizing beamsplitter. This apparatus embodies the transformation described in Equation 4.12 for photons. . . . . 30



# Acknowledgments

I would like to thank everyone in the Department of Physics at Harvey Mudd College for their patience and guidance over the past four years. Their excellent professorship has opened my eyes to a wide array of ideas in physics, and their ability to make complex topics seem simple leaves me something to aspire to personally. In particular, I would like to thank Theresa Lynn for her advice both in physics and in life, and for helping me through this thesis work. I also want to acknowledge the help of Michael Orrison and Dmitri Skjorshammer, who were always eager to bounce ideas around. Finally, I would like to thank all of my friends and family who have supported me, and Sarah Smilkstein especially, as I graduate and continue to pursue my passion in physics.



# Chapter 1

## Introduction

This thesis presents new theoretical bounds on Bell-state distinguishability using linear devices constrained to local measurement. The *Bell states* are a set of basis states used to describe entanglement between two particles (see Chapter 2 for a complete discussion of entanglement). In the emerging field of quantum information science, entangled states play a crucial role in many promising applications of quantum mechanics to tasks involving communication and/or computation. But a practical implementation of these quantum information protocols requires creating, measuring, and manipulating entangled states in the Bell basis. Physicists have made astounding progress in experimental techniques to generate pairs of entangled particles, but *measuring* entangled states has always been limited for so-called “linear evolution, local measurement” (LELM) devices. Linear evolution means that the detection apparatus acts on each particle independently from the state or evolution of the other, and local measurement means that each particle is localized at a particular detector registering a “click” to indicate that a particle has been detected.

The well-established no-go theorem limiting Bell-state distinguishability for LELM devices shows specifically that one cannot distinguish between more than three “classes” of Bell states for systems entangled in a single two-state variable [1]. Because there are a total of four Bell states and only three distinguishable classes, one class must contain at least two Bell states<sup>1</sup>. If a measurement result falls in this ambiguous class, we cannot differentiate between the two possibilities and hence a complete, deterministic Bell-state measurement is impossible for devices operating under LELM (see Figure 1.1).

---

<sup>1</sup>This follows from a straight-forward application of the pigeonhole principle.

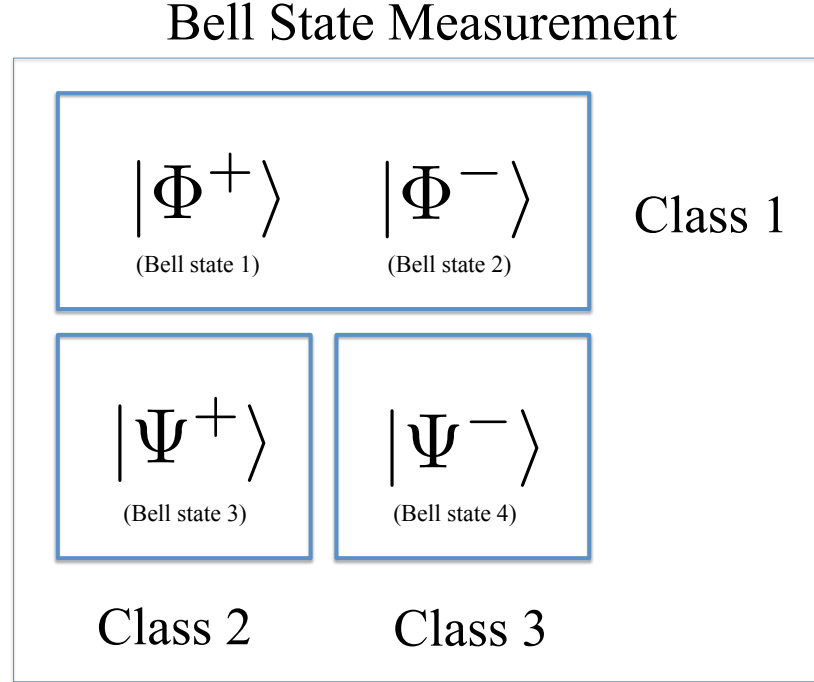


**Figure 1.1** *Breakdown of Bell-state classes.* A linear evolution, local measurement device can differentiate between at most three separate Bell-state classes. Here, a division of the four Bell states into different classes demonstrates how 50% of the time one will measure a state in Class 1 and hence make an ambiguous measurement. This limits the efficiency of applications such as quantum teleportation, which require an unambiguous measurement to succeed.

This limitation on Bell-state measurements made with LELM devices has real-world consequences for many quantum information protocols [2–4]. For example, consider the implications in quantum teleportation [5]. The goal of a successful teleportation is to take some particle  $Q$  (in a potentially unknown state) and reproduce it exactly at a distant location. We cannot simply measure  $Q$  directly, because any attempt to measure it would irreversibly destroy the original state while failing to reveal the complete set of information necessary to reproduce it elsewhere. However, we can measure  $Q$  indirectly by projecting it into an entangled state with some other particle  $A$  that is also entangled with a third particle  $B$  located at the destination. This projection is achieved via Bell-state measurement between particles  $Q$  and  $A$ , but successfully completing the teleportation requires

knowing exactly *which* Bell state is measured! An ambiguous result from an LELM apparatus means a failed teleportation. This protocol and others relying on Bell-state measurements are discussed in more detail in Chapter 3.

Reliable teleportation opens up a number of extremely exciting applications. For example, teleportation can be used to securely communicate information encoded in the state of particle  $Q$ . Not only does the sender not need to know the message to send it successfully, but the information encoded on  $Q$  itself never really “exists” anywhere before it is reconstructed at the destination. Hence, the message cannot be intercepted by an eavesdropper. Teleportation also has applications in quantum computing, where one must manipulate quantum states while preserving entanglement properties with other qubits in the system. The primary theoretical barrier that prohibits efficient realizations of these applications lies in making that unambiguous Bell-state measurement. With conventional LELM devices, unambiguous Bell-state discrimination is only possible for 50% of the attempted measurements, because the other 50% result in a class with two Bell states as illustrated schematically in Figure 1.1 [1].

Despite this fundamental limitation for LELM devices, physicists have invented methods that use entanglement in *two* variables to distinguish between all four Bell states in a single variable [6]. Heuristically, these *hyper-entangled systems* allow the experimenter to use known entanglement information about one of the variables to make a complete Bell-state measurement on the other. In a sense, the single-variable Bell-state measurement is embedded in a higher-dimensional space, which allows one to circumvent some of the limitations in LELM measurements. The potential for hyper-entangled states to improve existing quantum information protocols demands a thorough theoretical understanding of the limits on Bell-state measurements for systems entangled in many variables. Existing work has treated hyper-entangled systems in up to two degrees of freedom, and this thesis extends such results to an arbitrary  $n$  degrees of freedom. I derive an upper limit to the number of distinguishable classes of hyper-entangled Bell states in  $n$  degrees of freedom using linear evolution, local measurement devices. I also prove that there is a minimum size to any such Bell-state class, which limits the possible Bell-state resolution within a particular detection outcome.

The remaining chapters divide themselves as follows: Chapter 2 provides the necessary theoretical background for understanding hyper-entangled states, and explains most of the terminology used in later chapters. Chapter 3 motivates this work by discussing several real-world applica-

tions of Bell-state measurements, focusing on quantum teleportation in particular. Chapter 4 frames the problem in more detail and discusses previous work done on theoretical limits for Bell-state measurements. Chapters 5 and 6 constitute the main work of this thesis, proving the maximum number of distinguishable Bell-state classes for entanglement in  $n$  variables (Chapter 5) and the best-case resolution within a given Bell-state class (Chapter 6). Finally, Chapter 7 ties everything together and discusses further avenues for investigation.

The results presented here are theoretical limitations with practical consequences. They say something fundamental about measuring entanglement (a peculiar quantum phenomenon) with devices that are linear and inherently unentangling. Hopefully this thesis will help guide further research into applications of quantum mechanics and entanglement to information-theoretic tasks.

## Chapter 2

# Entanglement and the Bell Basis

### 2.1 Introduction

Classically speaking, digital logic and computing applications rely on binary representations of data in which each bit (or *state*) can either be a one or a zero. In digital circuits, these bits are represented by a high or a low voltage, respectively, but each bit is still presumed to represent a distinct state; as with Boolean algebra, a bit can either be a one or a zero, but not both. Quantum mechanics, however, allows for superpositions that do not occur classically. By analogy, we talk about a *qubit*, or *quantum-bit*, as some two-level system with eigenstates designated by  $|0\rangle$  and  $|1\rangle$ . As a quantum system, this qubit isn't restricted to the classically disjoint "zero or one" required by ordinary digital logic. Instead, a qubit can be in a superposition of its two eigenstates, and only upon measurement do we "read out" a discrete value. The advantage of superposition in applications such as quantum computing is that a single system of  $n$  qubits can be prepared in a superposition of all  $2^n$  possible states, allowing massively parallel computations to be made using quantum algorithms.

An arbitrary qubit state  $|q\rangle$  can be expressed as a generic superposition of its two eigenstates

$$|q\rangle = \alpha|0\rangle + \beta|1\rangle \quad (2.1)$$

where the coefficients  $\alpha$  and  $\beta$  are normalized probability amplitudes such that  $|\alpha|^2 + |\beta|^2 = 1$ . These qubit states form the basis of all quantum computation, and can theoretically be implemented in any two-level system.

The real advantage to using qubits in computation and communication-related tasks arises from another distinctly non-classical phenomenon known as *entanglement*. Entanglement is arguably the single most bizarre result to emerge from quantum mechanics. Einstein famously called it “spooky action at a distance” in an attempt to describe how spatially separated particles can be perfectly correlated in non-commuting observables, where the correlation is independent of which observable we decide to measure and how far apart the particles are when the measurement is made. Indeed, this is the crux of the famous EPR ‘paradox,’ which Einstein, Podolsky, and Rosen hoped would show that quantum mechanics cannot be complete [7]. Instead, it served to illustrate an entirely new quantum phenomenon with applications to almost all areas of quantum information science. Only in the last few decades have physicists really started to unentangle this bizarre result in terms of its practical applications, which promise to herald an entirely new era of computing and communication.

What, then, is entanglement? In simple terms, one might say that a pair of entangled particles know their relationship to each other better than they know their own state. That is, entanglement extends the notion of superposition to systems of multiple particles, in which no particle is in a definite state yet the *relationship* between the possible states for each particle is well-defined—knowing the state of one particle immediately determines the state of the other. In a system of two entangled particles, it is only necessary to measure one member of the pair *in any basis* to project the other into an exactly identical or exactly opposite state. It is one of the more unsettling but also one of the most intriguing aspects of entanglement that this wavefunction collapse occurs instantaneously over spacelike-separated intervals. How does a particle instantaneously “know” what state its partner is in? Could it actually be that the entangled particles really had definite states to begin with, and we were just unable to measure them?

For a number of years, this was an open question. Einstein, Podolsky, and Rosen favored such a “hidden-variable” formulation, but in 1964 John S. Bell published a theorem showing any local, hidden-variable description of reality to be “incompatible with the statistical predictions of quantum mechanics” [8]. In other words, a local realist interpretation of physics in which entangled particles really *do* have definite (although inaccessible) states is testable against the predictions of quantum mechanics. The famous Bell inequality that resulted from this paper was picked up a few years later by Clauser, Horne, Shimony, and Holt (CHSH), who derived a parallel result accounting for certain experimental realities left out of Bell’s derivation [9]. Their paper suggested a relatively straight-forward



experiment to differentiate between quantum mechanics and local realism, and the subsequent results confirm quantum mechanics to dizzying significance [10–12]. In one recent experiment, the threshold for local realism was violated by 1239 standard deviations. The probability that this is a statistical fluke is on the order of one part in  $10^{10^6}$  [13]! While there is still debate in some circles about possible loopholes in these Bell inequality experiments, the unsettling implications of entanglement have been demonstrated to the thorough satisfaction of most scientists in the physics community.

The remainder of this chapter discusses the theoretical background for entangled two-particle states. I define the basis most commonly used to describe entanglement (called the Bell basis in honor of John S. Bell), and generalize traditional discussions of entanglement to describe entanglement between two particles in an *arbitrary* number of variables. These ideas will be used repeatedly in later chapters to obtain theoretical bounds on our ability to distinguish between such non-local, entangled states using inherently linear, local measurement devices.

## 2.2 Mathematical foundation

Formally speaking, two particles are said to be entangled if their combined state cannot be written as a tensor product of states involving each particle individually. For example, consider two particles which we'll label  $L$  and  $R$  (for Left and Right, a notation which will become clear in later chapters). An *entangled state* of these two particles cannot be factored into a single tensor product between  $L$ -particle states and  $R$ -particle states. That is, the overall joint-particle state  $|\Psi_{LR}\rangle$  is entangled if

$$|\Psi_{LR}\rangle \neq |\psi_L\rangle \otimes |\phi_R\rangle \quad (2.2)$$

where  $|\psi_L\rangle$  and  $|\phi_R\rangle$  are generic states of the left and right particles individually. In general, I will use capital letters to designate joint-particle states (that is, states of two particles) and lower case letters to designate single-particle states (that is, states involving *either* particle L *or* particle R, with additional subscripts to clarify which is meant).

Let's consider a few examples to help spell out this idea of entanglement. Imagine a pair of particles characterized by some variable with two discrete eigenstates. For the sake of generality, we represent these eigenstates in the binary basis as  $\{|0\rangle, |1\rangle\}$ . However, the binary basis states are simply a stand-in for the eigenstates of any two-level system. For example, with photons we might consider polarization entanglement, in which case

the basis would be  $\{|H\rangle, |V\rangle\}$  for linear polarization or  $\{|L\rangle, |R\rangle\}$  for circular polarization. We might also consider entanglement in variables such as orbital angular momentum, in which case we restrict ourselves to the subset  $\{|+\hbar\rangle, |-\hbar\rangle\}$  or any equivalent two-element list of orbital angular momentum states. Similarly, we might consider eigenstates of linear momentum, in which case we would use a subset  $\{a, b\}$  of possible linear momentum states that can be discretely measured. For electrons, examples include the set of spin states  $\{|\uparrow_z\rangle, |\downarrow_z\rangle\}$  or two ground/meta-stable states in an atom.

An example of an entangled state  $|\Psi_{LR}\rangle$  is given by

$$|\Psi_{LR}\rangle = \frac{1}{\sqrt{2}}(|0\rangle_L|1\rangle_R + |1\rangle_L|0\rangle_R) \quad (2.3)$$

This clearly cannot be separated into a product of  $L$ - and  $R$ -particle states, where the general  $L$ - and  $R$ -particle states both take the form of an arbitrary qubit,  $|\psi_L\rangle = \alpha_L|0\rangle_L + \beta_L|1\rangle_L$  or  $|\phi_R\rangle = \alpha_R|0\rangle_R + \beta_R|1\rangle_R$ . Thus, the state in Equation (2.3) is entangled. For contrast, consider another state  $|\Psi_{LR}\rangle$  given by

$$|\Psi_{LR}\rangle = \frac{1}{\sqrt{2}}(|0\rangle_L|1\rangle_R + |1\rangle_L|1\rangle_R) \quad (2.4)$$

This can be factored as

$$|\Psi_{LR}\rangle = \frac{1}{\sqrt{2}}(|0\rangle_L + |1\rangle_L)|1\rangle_R \quad (2.5)$$

which is not entangled because we quickly identify

$$\begin{aligned} |\psi_L\rangle &= \frac{1}{\sqrt{2}}(|0\rangle_L + |1\rangle_L) \\ |\phi_R\rangle &= |1\rangle_R \end{aligned} \quad (2.6)$$

such that the original state in Equation (2.4) can be written as a single tensor product  $|\Psi_{LR}\rangle = |\psi_L\rangle \otimes |\phi_R\rangle$ .

Intuitively speaking, entangled states are non-local. That is, the state of one particle depends on the spatially-separated state of the other, but neither particle has a definite state until one of them is measured. When one of the particles *is* measured, the entire system collapses instantaneously into perfectly correlated eigenstates, even if the two particles are space-like separated. It is tempting to think this could lead to faster-than-light communication, but entanglement only manifests itself when a correlation

comparison is made between the two particles. Observing a single particle in isolation would lead to completely random measurements of that particular observable; because we cannot control which eigenstate the system collapses to, there cannot be any purposeful communication using only the entangled quantum channel.

Based on the examples above, intuition might suggest that one way of quantifying entanglement is to consider the minimum number of tensor product terms required to write the entangled state. This intuition is rigorously embodied in the idea of a Schmidt number. Mathematically speaking, the Schmidt number is the number of terms in the Schmidt decomposition of the state's density matrix. Entangled states have a Schmidt number of at least two, because (by definition) they cannot be factored into a single tensor product term between states of separate particles [14]. The example states given in Equations (2.3) and (2.4) illustrate this idea; there is no way to write Equation (2.3) as a single tensor product term, unlike the state in Equation (2.4) which is not entangled and can easily be manipulated into the single tensor product term given in Equation (2.5).

## 2.3 The Bell Basis and Hyper-entangled states

### 2.3.1 Entanglement in a single variable

The Bell basis is well-suited for discussions of entanglement, and is represented by the set of four maximally-entangled two-qubit states given by

$$\begin{aligned}
 |\Phi^+\rangle &= \frac{1}{\sqrt{2}} \left( |0\rangle_L |0\rangle_R + |1\rangle_L |1\rangle_R \right) \\
 |\Phi^-\rangle &= \frac{1}{\sqrt{2}} \left( |0\rangle_L |0\rangle_R - |1\rangle_L |1\rangle_R \right) \\
 |\Psi^+\rangle &= \frac{1}{\sqrt{2}} \left( |0\rangle_L |1\rangle_R + |1\rangle_L |0\rangle_R \right) \\
 |\Psi^-\rangle &= \frac{1}{\sqrt{2}} \left( |0\rangle_L |1\rangle_R - |1\rangle_L |0\rangle_R \right)
 \end{aligned} \tag{2.7}$$

These basis states divide themselves structurally into two classes, defined by the choice of  $\Phi$  versus  $\Psi$ . (The choice of  $\pm$  in the superscript simply corresponds to the phase of the superposition.) The  $\Phi$  Bell states describe particles that are perfectly correlated in the  $|0\rangle/|1\rangle$  basis, while the  $\Psi$  Bell states describe particles that are perfectly anti-correlated in the  $|0\rangle/|1\rangle$  basis. In other words, a pair of entangled particles in a  $\Phi$  Bell state will al-

ways collapse to the *same* eigenstate when measured in this basis (although which eigenstate is measured is completely random), while particles in a  $\Psi$  Bell state will always collapse to *opposite* eigenstates when measured in this basis. These four states span the space of all two-qubit states, and their maximally entangled nature makes them ideal for discussing entanglement.

In later chapters, it will sometimes be convenient to represent a two-particle system in both the Bell basis and the basis of unentangled, joint-particle states given by

$$\{ |0\rangle_L |0\rangle_R, |1\rangle_L |1\rangle_R, |0\rangle_L |1\rangle_R, |1\rangle_L |0\rangle_R \} \quad (2.8)$$

From the Bell-basis states in Equation (2.7), we form the matrix  $\mathbf{M}_0$  where

$$\begin{pmatrix} |\Phi^+\rangle \\ |\Phi^-\rangle \\ |\Psi^+\rangle \\ |\Psi^-\rangle \end{pmatrix} = \mathbf{M}_0 \begin{pmatrix} |0\rangle_L |0\rangle_R \\ |1\rangle_L |1\rangle_R \\ |0\rangle_L |1\rangle_R \\ |1\rangle_L |0\rangle_R \end{pmatrix}; \quad \mathbf{M}_0 = \frac{1}{\sqrt{2}} \begin{pmatrix} 1 & 1 & 0 & 0 \\ 1 & -1 & 0 & 0 \\ 0 & 0 & 1 & 1 \\ 0 & 0 & 1 & -1 \end{pmatrix} \quad (2.9)$$

Any state vector represented in the (unentangled) joint-particle basis can be easily rotated into the Bell basis and vice versa by applying the unitary transformation matrix  $\mathbf{M}_0$ .

### 2.3.2 Hyper-entangled Bell states

Hyper-entanglement, simply stated, is entanglement between two particles in multiple qubit variables [15]. To use an experimentally versatile example, the nonlinear process of spontaneous parametric downconversion creates two photons entangled in polarization, orbital angular momentum (OAM), linear momentum, and energy [16]. Restricting ourselves to a subset of two eigenstates for variables such as OAM, linear momentum, and energy, we recover the structure of a qubit in all of these variables and thus can leverage the formalism described above.

The hyper-entangled Bell states are constructed from the single-variable Bell states defined in Equation (2.7). For entanglement in  $n$  qubit degrees of freedom, the complete hyper-entangled Bell basis is constructed by forming all possible tensor products of Bell states in the individual variables. For example,

$$|B_{123\dots}\rangle = |\Phi_1^+\rangle \otimes |\Psi_2^-\rangle \otimes |\Psi_3^+\rangle \otimes \dots \quad (2.10)$$

is one such hyper-entangled Bell state, where each individual variable  $\{1, 2, 3, \dots\}$  is in the Bell state  $\{\Phi^+, \Psi^-, \Psi^+, \dots\}$ , respectively. Just as a

single-variable entangled state can be represented in either the entangled Bell basis or the unentangled basis of joint-particle states, hyper-entangled states can also be represented in both bases. For generalized  $n$  degrees of freedom, the relationship between the Bell basis and the unentangled, joint-particle basis is carried in the unitary transformation matrix  $\mathbf{M}_n$  given by

$$\mathbf{M}_n = \mathbf{M}_0^{\otimes n} \quad (2.11)$$

In linear algebra terms,  $\mathbf{M}_n$  is constructed by taking sequential Kronecker products (defined below) between  $n$  copies of  $\mathbf{M}_0$ , thereby casting the higher-dimensional tensor product space in matrix form. The matrix  $\mathbf{M}_n$  is thus a generalization of Equation (2.9) to an arbitrary  $n$  degrees of freedom.

In this thesis, the  $n = 1$  unentangled joint-particle basis is ordered as

$$\{ |0\rangle_L |0\rangle_R, |1\rangle_L |1\rangle_R, |0\rangle_L |1\rangle_R, |1\rangle_L |0\rangle_R \} \quad (2.12)$$

The Kronecker product structure used to define  $\mathbf{M}_n$  in Equation (2.11) implies a similarly ordered basis for  $n > 1$ . To see how this basis scales to larger  $n$ , we first look at how the Kronecker product is defined between two matrices  $\mathbf{A}$  and  $\mathbf{B}$ :

$$\mathbf{A} \otimes \mathbf{B} = \begin{bmatrix} a_{11}B & \cdots & a_{1n}B \\ \vdots & \ddots & \vdots \\ a_{n1}B & \cdots & a_{nn}B \end{bmatrix} \quad (2.13)$$

In essence, the Kronecker product works by taking each element of  $\mathbf{A}$ , multiplying it by the entire matrix  $\mathbf{B}$ , and embedding the result as a submatrix in  $\mathbf{A} \otimes \mathbf{B}$ . Following this rule, we see that the  $n = 2$  basis must have the ordering

$$\begin{aligned} & |00\rangle_L |00\rangle_R, |01\rangle_L |01\rangle_R, |00\rangle_L |01\rangle_R, |01\rangle_L |00\rangle_R, \\ & |10\rangle_L |10\rangle_R, |11\rangle_L |11\rangle_R, |10\rangle_L |11\rangle_R, |11\rangle_L |10\rangle_R, \\ & |00\rangle_L |10\rangle_R, |01\rangle_L |11\rangle_R, |00\rangle_L |11\rangle_R, |01\rangle_L |10\rangle_R, \\ & |10\rangle_L |00\rangle_R, |11\rangle_L |01\rangle_R, |10\rangle_L |01\rangle_R, |11\rangle_L |00\rangle_R \end{aligned} \quad (2.14)$$

This can be broken down into four blocks (separated onto individual lines above), where each block takes a single state from our  $n = 1$  basis to use as the first variable and combines it with every state from that basis as the second variable. Thus, the first row in Equation (2.14) contains all states with  $|0\rangle_L |0\rangle_R$  for the first variable, and as we move *across* the row we see

that the second variable assumes every state from the basis given in Equation (2.12). The second, third, and fourth rows repeat this pattern in the remaining basis states for the first variable.

In the interest of completeness it is worth noting quickly that the two-particle,  $n$ -variable state space has dimension  $4^n$ ; thus both the unentangled basis of Equation (2.14) and the hyper-entangled Bell basis are made up of  $4^n$  basis states. It is also worth emphasizing that the hyper-entangled Bell basis expresses entanglement between spatially distinct qubits. It is possible to consider states that exhibit entanglement between *variables* of a given particle, but this thesis and the relevant applications focus on two-particle entanglement and so we will not concern ourselves with cross-variable entangled states.

## 2.4 $\Phi/\Psi$ Signatures

In Section 2.3.1 above, I describe how the Bell states naturally divide themselves into classes separated by the choice of  $\Phi$  versus  $\Psi$ . Extending this idea to multiple degrees of freedom, we construct equivalence classes of hyper-entangled Bell states represented by a particular  $\Phi/\Psi$  *signature*. More specifically, we divide the Bell states according to whether they are in a  $\Phi$  or a  $\Psi$  Bell-state class for each individual variable, and the resulting list of  $\Phi$ 's and  $\Psi$ 's make up that state's  $\Phi/\Psi$  signature. For example, the state

$$|B_{123}\rangle = |\Phi_1^+\rangle \otimes |\Psi_2^-\rangle \otimes |\Psi_3^+\rangle \quad (2.15)$$

has a  $\Phi/\Psi$  signature  $\{\Phi, \Psi, \Psi\}$ . Similarly, the state

$$|B'_{123}\rangle = |\Psi_1^+\rangle \otimes |\Phi_2^-\rangle \otimes |\Psi_3^+\rangle \quad (2.16)$$

has a  $\Phi/\Psi$  signature  $\{\Psi, \Phi, \Psi\}$ . Experimentally speaking, it is straightforward to determine the  $\Phi/\Psi$  signature of a given state. All one has to do is perform a projective measurement on each particle in the  $|0\rangle/|1\rangle$  basis for all  $n$  variables, and examine the correlation/anti-correlation properties between the two particles. If the two particles are correlated (*i.e.*, in the same eigenstate) for a particular variable, then write down a  $\Phi$  for that variable in the state's  $\Phi/\Psi$  signature. If the two particles are anti-correlated (*i.e.*, in opposite eigenstates), write down a  $\Psi$ . Conversely, knowledge of a state's  $\Phi/\Psi$  signature is enough to reconstruct the correlation relationships between single-variable eigenstates of each qubit. By a simple counting argument, there are  $2^n$   $\Phi/\Psi$  signatures, and each signature defines an equivalence class between  $2^n$  hyper-entangled Bell states. This concept will be useful for the proofs presented in Chapters 5 and 6.

As a final aside, the structure of the Bell states in a single variable generalizes the singlet/triplet division in systems of two spin-1/2 particles. The set of three triplet states for two non-identical fermions (such as the proton-electron state in hydrogen) are given by [17]:

$$|1, 1\rangle = | + z \rangle_1 | + z \rangle_2 \quad (2.17)$$

$$|1, 0\rangle = \frac{1}{\sqrt{2}} | + z \rangle_1 | - z \rangle_2 + \frac{1}{\sqrt{2}} | - z \rangle_1 | + z \rangle_2 \quad (2.18)$$

$$|1, -1\rangle = | - z \rangle_1 | - z \rangle_2 \quad (2.19)$$

and the singlet state is

$$|0, 0\rangle = \frac{1}{\sqrt{2}} | + z \rangle_1 | - z \rangle_2 - \frac{1}{\sqrt{2}} | - z \rangle_1 | + z \rangle_2 \quad (2.20)$$

We see immediately that

$$|1, 1\rangle \xrightarrow{S_z} \frac{1}{\sqrt{2}} |\Phi^+\rangle + \frac{1}{\sqrt{2}} |\Phi^-\rangle \quad (2.21)$$

$$|1, 0\rangle \xrightarrow{S_z} |\Psi^+\rangle \quad (2.22)$$

$$|1, -1\rangle \xrightarrow{S_z} \frac{1}{\sqrt{2}} |\Phi^+\rangle - \frac{1}{\sqrt{2}} |\Phi^-\rangle \quad (2.23)$$

while

$$|0, 0\rangle \xrightarrow{S_z} |\Psi^-\rangle \quad (2.24)$$

If we re-express Equations (2.17)–(2.20) in the  $S_x$  basis, however, we find that

$$|1, 1\rangle \xrightarrow{S_x} \frac{1}{\sqrt{2}} |\Phi^+\rangle + \frac{1}{\sqrt{2}} |\Psi^+\rangle \quad (2.25)$$

$$|1, 0\rangle \xrightarrow{S_x} |\Phi^-\rangle \quad (2.26)$$

$$|1, -1\rangle \xrightarrow{S_x} \frac{1}{\sqrt{2}} |\Phi^+\rangle - \frac{1}{\sqrt{2}} |\Psi^+\rangle \quad (2.27)$$

while

$$|0, 0\rangle \xrightarrow{S_x} -|\Psi^-\rangle \quad (2.28)$$

The interesting aspect of this structure is that the set of triplet states is closed under change of basis, while the singlet state is basis-independent and thus forms a closed set as well under this operation. For the Bell states, we find that  $|\Psi^-\rangle$  behaves like the  $|0, 0\rangle$  singlet in that its form is also basis-independent, while the other three Bell states  $|\Phi^+\rangle$ ,  $|\Phi^-\rangle$ , and  $|\Psi^+\rangle$  behave like the spin-1/2 triplet states and form a closed set under change of basis. This division of the Bell states is isomorphic to the division between singlet and triplet states in systems of spin-1/2 particles. The distinguishing characteristic between the singlet state  $|\Psi^-\rangle$  and the other states is that  $|\Psi^-\rangle$  is anti-symmetric under exchange of spatial channels whereas the others are symmetric. This anti-symmetry in  $|\Psi^-\rangle$  will play an important role later in defining Bell-state classes that result from linear evolution and local projective measurements.

Now that we have a solid understanding of Bell states and the hyper-entangled Bell basis, we will move on to the next chapter which motivates this thesis by discussing how Bell-state measurements are applied in various quantum information protocols.



## Chapter 3

# Protocols Relying on Bell-state Discrimination

### 3.1 Introduction

Entanglement plays a crucial role in many real-world applications of quantum mechanics. However, two major experimental barriers must be addressed before these applications can have any practical benefit. First and perhaps most obviously, we must develop a robust method to generate pairs of entangled particles, and depending on the application, it may also be necessary to generate them in a particular entangled state. The second hurdle involves devising an equally robust method to *measure* entangled states.

While the first challenge is by no means trivial, substantial progress has been made towards generating entangled particles in arbitrary Bell states. For example, entangled photons are readily produced in particular Bell states through the non-linear interactions of spontaneous parametric downconversion (SPDC) [16]. This “ultra-bright source” of entangled photons has proven extremely useful in a wide array of experiments and proof-of-concept applications ranging from quantum cryptography to quantum computing. Additionally, SPDC has made it possible to rigorously investigate certain fundamental questions in quantum mechanics, such as the question of local realism and Bell’s inequalities discussed in Chapter 2.

Yet despite such progress, many quantum information protocols also hinge on our ability to make unambiguous and/or deterministic Bell-state measurements. For example, successful quantum teleportation (discussed below) requires an unambiguous measurement to be made in the Bell ba-

sis. This chapter discusses several protocols relying on Bell-state measurements, placing particular emphasis on teleportation as the canonical example. These applications serve to motivate the rest of the thesis, which addresses theoretical limitations on Bell-state measurements using linear evolution, local measurement (LELM) devices. The exact nature of these limitations has implications for our ability to implement the protocols discussed below.

## 3.2 Quantum Teleportation

The Oxford English Dictionary defines *teleportation* as the “apparently instantaneous transportation of persons, etc., across space by advanced technological means” [18]. “Teleportation” as depicted in shows like *Star Trek* may seem sexier than teleportation as discussed in quantum information science, but the core idea is the same. Information is encoded on a qubit, and the goal is to teleport the state of that particle to a co-conspirator who can then extract any relevant information. But unlike teleportation in science fiction, relativistic restrictions on causality prevent information from traveling faster than the speed of light; unfortunately, teleportation cannot be instantaneous. Instead, the teleportation process is split into a “quantum” step and a “classical” step. The classical step involves broadcasting the result of a Bell-state measurement to the destination, but does not divulge any information about the state being teleported. Instead, the result of the Bell-state measurement is used by one’s co-conspirator to *reconstruct* the original state from half of an entangled pair (the “quantum channel”) that is shared between the two ends. Quantum teleportation harnesses the non-local nature of entanglement such that the qubit is dematerialized at the input and rematerialized at the output without ever “existing” in between. Thus, teleportation can be used to securely transmit information without the risk of interception by an eavesdropper.

### 3.2.1 Technical description

Charles Bennett, *et al.* published the details of this protocol in a 1993 paper in *Physical Review Letters* [5]. The idea is as follows: An entangled pair of particles (often called an *EPR pair*) is created in the  $|\Psi^-\rangle$  singlet state, and Alice (the sender) keeps one half of the pair while Bob (the receiver) keeps the other half. This entangled EPR singlet serves as the “quantum channel” in the teleportation procedure. Now, say Alice receives a qubit in some ar-

bitrary state, which she must teleport to Bob. To do so, she projects her half of the EPR pair and the qubit  $Q$  into an entangled Bell state by performing a measurement on the two particles in the Bell basis. She broadcasts the result of her measurement (via some classical channel) to Bob, who then performs one of four simple state transformations on his half of the EPR pair to reconstruct the original state of  $Q$ . This process is represented schematically in Figure 3.1.

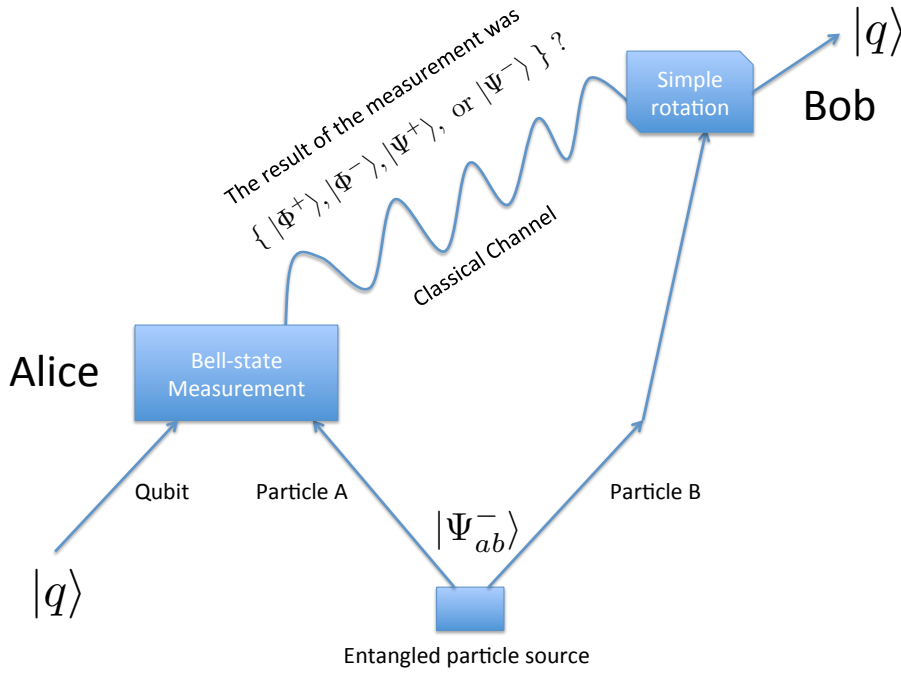


**Figure 3.1** *Schematic of a quantum teleportation device.* Alice and Bob each possess one member of an EPR pair in the singlet state  $|\Psi^- \rangle$ . To teleport the state of some particle  $Q$ , Alice performs a Bell-state measurement between  $Q$  and her half of the entangled pair. She broadcasts the result to Bob via some classical channel, who then performs one of four simple transformations given by Equations (3.10)–(3.13) on his particle to recover the original state of  $Q$ .

To see how this works mathematically, consider two particles  $A$  and  $B$  in the EPR singlet state

$$|\Psi^-_{ab}\rangle = \frac{1}{\sqrt{2}} \left( |0\rangle_a |1\rangle_b - |1\rangle_a |0\rangle_b \right) \quad (3.1)$$

Similarly, consider some qubit particle  $Q$  in the state

$$|q\rangle = \alpha|0\rangle_q + \beta|1\rangle_q \quad (3.2)$$

which Alice wishes to teleport. Here, the subscripts and names of the particles in the EPR state refer to Alice ( $a$ ) and Bob ( $b$ ), and  $q$  for Qubit. For the purpose of this derivation we are assuming  $Q$  to be in the pure state given by Equation (3.2), but it does not have to be. For example,  $Q$  might be entangled with some other set of particles not involved in the teleportation, but after  $Q$  is successfully teleported, the new particle at the destination will possess all entanglement properties originally held by  $Q$ .

To actually teleport the qubit state, Alice needs to first perform a projective measurement in the Bell-state basis between her particle  $A$  and the qubit  $Q$ . The complete three-particle state  $|\Psi_{ab}^-\rangle|q\rangle$  can be factored and rewritten in terms of Bell states of  $Q$  and  $A$ , such that a Bell-basis measurement between  $Q$  and  $A$  will project Bob's particle into some state  $|b\rangle$  that is related to the original qubit state  $|q\rangle$  by a simple transformation. To see this, we first write the total state  $|\Psi_{ab}^-\rangle|q\rangle$  and expand to get

$$\begin{aligned} |\Psi_{ab}^-\rangle|q\rangle &= \frac{1}{\sqrt{2}}(|0\rangle_a|1\rangle_b - |1\rangle_a|0\rangle_b) (\alpha|0\rangle_q + \beta|1\rangle_q) \\ &= \frac{1}{\sqrt{2}}(\alpha|0\rangle_q|0\rangle_a|1\rangle_b - \alpha|0\rangle_q|1\rangle_a|0\rangle_b + \beta|1\rangle_q|0\rangle_a|1\rangle_b - \beta|1\rangle_q|1\rangle_a|0\rangle_b) \end{aligned} \quad (3.3)$$

We can easily rewrite products between particles  $Q$  and  $A$  in the Bell basis, using the fact that

$$|0\rangle_q|0\rangle_a = \frac{1}{\sqrt{2}}(|\Phi_{qa}^+\rangle + |\Phi_{qa}^-\rangle) \quad (3.4)$$

$$|1\rangle_q|1\rangle_a = \frac{1}{\sqrt{2}}(|\Phi_{qa}^+\rangle - |\Phi_{qa}^-\rangle) \quad (3.5)$$

$$|0\rangle_q|1\rangle_a = \frac{1}{\sqrt{2}}(|\Psi_{qa}^+\rangle + |\Psi_{qa}^-\rangle) \quad (3.6)$$

$$|1\rangle_q|0\rangle_a = \frac{1}{\sqrt{2}}(|\Psi_{qa}^+\rangle - |\Psi_{qa}^-\rangle) \quad (3.7)$$

which are easily derived from Equation (2.7). Substituting these into Equation (3.3) gives us an alternative representation of the complete three-particle

state in terms of particle  $B$  and Bell states of particles  $Q$  and  $A$ :

$$|\Psi_{ab}^-\rangle|q\rangle = \frac{1}{2} \left[ (|\Phi_{qa}^+\rangle + |\Phi_{qa}^-\rangle)\alpha|1\rangle_b - (|\Psi_{qa}^+\rangle + |\Psi_{qa}^-\rangle)\alpha|0\rangle_b \right. \\ \left. + (|\Psi_{qa}^+\rangle - |\Psi_{qa}^-\rangle)\beta|1\rangle_b - (|\Phi_{qa}^+\rangle - |\Phi_{qa}^-\rangle)\beta|0\rangle_b \right] \quad (3.8)$$

$$= \frac{1}{2} \left[ |\Psi_{qa}^-\rangle(\alpha|0\rangle_b + \beta|1\rangle_b) - |\Psi_{qa}^+\rangle(\alpha|0\rangle_b - \beta|1\rangle_b) \right. \\ \left. + |\Phi_{qa}^-\rangle(\beta|0\rangle_b + \alpha|1\rangle_b) - |\Phi_{qa}^+\rangle(\beta|0\rangle_b - \alpha|1\rangle_b) \right] \quad (3.9)$$

When Alice makes a Bell-state measurement between the input qubit and her half of the EPR singlet, she projects  $Q$  and  $A$  into one of the entangled Bell states  $|\Phi_{qa}^+\rangle$ ,  $|\Phi_{qa}^-\rangle$ ,  $|\Psi_{qa}^+\rangle$ , or  $|\Psi_{qa}^-\rangle$ . She broadcasts the result of this measurement to Bob, who then performs one of the following transformations to his particle depending on the message he receives from Alice:

$$|\Psi^-\rangle \rightarrow \text{Identity} \quad (3.10)$$

$$|\Psi^+\rangle \rightarrow \begin{pmatrix} 1 & 0 \\ 0 & -1 \end{pmatrix} \quad (3.11)$$

$$|\Phi^-\rangle \rightarrow \begin{pmatrix} 0 & 1 \\ 1 & 0 \end{pmatrix} \quad (3.12)$$

$$|\Phi^+\rangle \rightarrow \begin{pmatrix} 0 & 1 \\ -1 & 0 \end{pmatrix} \quad (3.13)$$

After performing the appropriate transformation given in Equations (3.10)–(3.13), Bob has a particle that is in the same state as the original qubit  $Q$ . The teleportation is now complete!

It is worth emphasizing a few points. First, it is not necessary for Alice to know the state of  $Q$  in order to perform a successful teleportation. Additionally,  $Q$  might itself be entangled with other qubits, and the entanglement would transfer to  $B$  as mentioned previously. This fact has exciting implications for distributed quantum computing applications if the teleportation process can be reliably implemented.

The act of measuring  $Q$  and  $A$  in the Bell basis destroys the original qubit state  $|q\rangle$ , as is required by the no-cloning theorem [19; 20]. However, the benefit of this indirect measurement is that we can perfectly reconstruct  $|q\rangle$  at the destination without having to physically transport the particle  $Q$  itself. But Bob cannot be sure he has the original qubit  $Q$  until *after* he receives the result of Alice's Bell-state measurement and performs the necessary rotation to  $B$ . This is all in accordance with special relativity, as

information that might be encoded on  $Q$  cannot be transmitted faster than the speed of light. Teleportation is necessarily limited by the speed of the classical channel.

A final interesting observation is that unlike some forms of communication, Alice does not strictly need to know where Bob is located in order to teleport the qubit; she could broadcast her Bell-state results to all places Bob might be, and he can then make the appropriate transformation to his half of the (previously-shared) EPR pair to securely recreate the information sent by Alice. Such qualities make teleportation promising for applications that require secure communication.

### 3.3 Other protocols

Teleportation is often considered the canonical application of Bell-state measurement in quantum information science. However, there are numerous other applications which require the use of Bell-state measurements. For example, quantum dense coding is a protocol which aims to beat the channel capacity of traditional communication [3]. In this protocol, one selects a set of entangled Bell states as “code-words” to represent different symbols in a coded language. For  $n = 1$ , there are four Bell states meaning one might hope to send  $\log_2(4) = 2$  classical bits of information per qubit variable. Limitations on our ability to perform Bell-state measurements, however, mean limitations on the maximum possible channel capacity in a dense coding protocol. Other protocols that take advantage of Bell-state measurements include entanglement swapping [2; 21], fault tolerant quantum computing [22], and quantum repeaters [23].

Hopefully the applications discussed in this chapter have made it clear how useful unconditional Bell-state measurements can be. The remainder of this thesis is devoted to proving theoretical bounds on Bell-state measurements with linear evolution, local measurement devices. First, however, I must describe the mathematical framework used to discuss this problem. Chapter 4 establishes such a framework, and discusses previous results relating to distinguishability limits for Bell-state measurements using LELM devices.

## Chapter 4

# Setup and Previous Work

### 4.1 Introduction

In classical physics, the goal of “measurement” is to know or predict the state of a system without disturbing the system itself. As a philosophical aside, experimentation and by extension, measurement, are the only tools we have to differentiate between reality and what might be considered speculation or faith. Our ability to measure the world in a repeatable fashion is at the very bedrock of empirical science, and hence a fundamental understanding of measurement is essential to our understanding of science itself. This thesis addresses theoretical limitations on measurements of entangled particles, but before addressing that problem I want to put the idea of “measurement” in quantum mechanics into some context.

The loose definition of measurement suggested in the previous paragraph captures the intuition expressed by Einstein, Podolsky, and Rosen in their famous 1935 paper, *Can Quantum-Mechanical Description of Physical Reality Be Considered Complete?* [7]. They make the claim that if, “without in any way disturbing a system, we can predict with certainty... the value of a physical quantity, then there exists an element of physical reality corresponding to [that] physical quantity.” As one might expect, measurement is tied up in how we define reality itself. However, the concept of measurement that accords with our classical intuitions does not carry over into the quantum realm. Instead, quantum mechanics has shown us that measurement inherently disturbs the state of a system; what “really” happens during measurement is still an area of very active research, but developments in modern physics have required us to amend our classical understanding of measurement to apply in quantum systems.

The standard theoretical approach to the measurement process is embodied in so-called von Neumann projective measurements, named for the 20th century physicist and mathematician John von Neumann. While not crucial to understanding the results of this thesis, von Neumann measurements contribute to the theoretical underpinnings of the Bell-state measurement problem I solve in Chapters 5 and 6. Thus, I will outline the general idea for the sake of completeness<sup>1</sup>.

Consider some system in the (arbitrary) state  $|\psi\rangle$ . From a purely practical perspective, you can't just "look" at it and write down the results of your "observation." Instead, measurement involves somehow coupling the readout of a macroscopic laboratory device to the actual state of the microscopic system such that the classically accessible state of the laboratory instrument will reveal something about the state of the quantum system.

How might this coupling/readout process occur? Let's assume generally speaking that the laboratory instrument is a stand-in for some classically accessible "pointer" state  $|\phi\rangle$ . We make a measurement by interacting our quantum system  $|\psi\rangle$  with the pointer state  $|\phi\rangle$ , and wait for the entire system to evolve unitarily to some later time when we measure the value of the pointer. This measurement collapses the quantum system into a particular eigenstate corresponding to the value of the pointer.

Mathematically, this can be described as

$$|\psi\rangle_{\text{system}}|\phi\rangle_{\text{pointer}} \xrightarrow{\text{unitary evolution}} \sum_i c_i |\psi_i\rangle |\phi_i\rangle \quad (4.1)$$

The pointer could assume any eigenvalue from its basis of eigenstates, but whichever value is measured will cause the quantum system to collapse into the corresponding eigenstate. This measurement event destroys the original state  $|\psi\rangle$ , but immediately after the measurement is finished, our quantum system is in a definite state  $|\psi_i\rangle$  corresponding to the result  $|\phi_i\rangle$  of the pointer measurement.

The central focus of this thesis is to prove certain theoretical bounds on the distinguishability of hyper-entangled Bell states via measurements constrained by "linear evolution and local measurement" (LELM). For a variety of practical reasons, LELM devices are well-suited to quantum communication and quantum computing tasks. In particular, the emphasis on *linear evolution* comes from the fact that linear processes have much higher cross-sections than non-linear interactions. In other words, given two particles we are tasked to measure, the probability of achieving a successful

---

<sup>1</sup>This follows the approach of John Preskill in in [14].



measurement is much smaller for non-linear processes than for linear processes. Because linear devices do not rely on low-probability spatial coincidences and weak interactions between separate particles, they are virtually guaranteed to evolve the inputted system in a regular and predictable way for every attempted measurement.

The “local measurement” constraint of LELM is added almost as a necessary criterion. Generally speaking, we *measure* the existence of a particle by registering a click in some detector. This annihilation event projects that particle into a localized state, because we know it must have entered the detector to register a click. In the context of von Neumann measurements, the “pointer state” used here is the state of a detector after registering a click. Thus “local measurement” is included more or less for the sake of completeness, because it is a necessary criterion in most strategies to detect a microscopic entity. The real workhorse for the proofs presented in Chapters 5 and 6 is the linear evolution criterion, which is discussed in more detail in Section 4.2.

To build experimental intuition for what an LELM device might look like, again consider the example of photons. It has been shown that all LELM devices can be built from a series of mirrors, beam splitters, and wave plates [24]. The proof is achieved by decomposing the mathematical representation of an arbitrary LELM device into components that behave like mirrors, beam splitters, and phase shifters. As a consequence, this statement is applicable more generally to any system that can be manipulated using optical techniques. The point, however, is that LELM devices are typically easy to construct, explaining why they are emphasized for use in real-world quantum measurements.

The next section deals with the mathematical formalism used in this thesis to discuss LELM devices, followed by Section 4.3 which presents several relevant results from the literature.

## 4.2 Mathematical formalism

The most generic linear evolution apparatus can be thought of as a unitary, linear matrix transformation mapping some set of single-particle input states to a set of output states. The measurement process involves annihilating particles in some set of detectors at the output. To keep our discussion as general as possible, we consider annihilation in the Fock state basis, such that we can register (and count) multiple “clicks” in the same detection channel. We will see later that this type of “double-click” measurement

plays a special role in bounding the number of distinguishable Bell-state classes, but for now we will only concern ourselves with the mathematical structure describing such measurement outcomes.

What do these single-particle states look like for our system? Because we are interested in measurements over the set of hyper-entangled Bell states, our single-particle input states are simply the single-particle states of the hyper-entangled Bell basis. That is, they are the states  $\{|0\rangle, |1\rangle\}^{\otimes n}$  described by some set of eigenvalues for all  $n$  two-state variables under consideration. We can leverage the binary basis representation to write a particular state as a binary string of length  $n$ , where each digit corresponds to an eigenstate of a single two-state variable. For the purposes of measurement, we must additionally specify which spatial channel the particle enters the device through (either  $L$  for Left or  $R$  for Right). Thus, our space of single-particle input states has dimension  $2^{n+1}$ , where the additional factor of two comes from the  $L$ - versus  $R$ -channel specification.

Let's consider a concrete example. Say a particular photon is vertically polarized, is in an  $l = 1$  eigenstate of orbital angular momentum, and has a discretely characterized frequency  $\nu_1$ . We'll map these variables onto the binary basis states  $\{|0\rangle, |1\rangle\}$  as follows:

$$\begin{aligned} \{|H\rangle, |V\rangle\} &\rightarrow \{|0\rangle, |1\rangle\}_{\text{pol}} \\ \{|+\hbar\rangle, |-\hbar\rangle\} &\rightarrow \{|0\rangle, |1\rangle\}_{\text{OAM}} \\ \{|\nu_1\rangle, |\nu_2\rangle\} &\rightarrow \{|0\rangle, |1\rangle\}_{\text{freq}} \end{aligned} \tag{4.2}$$

In the binary basis, this photon is easily described as  $|100\rangle$ , where we have ordered our variables in the same order they are listed above. The set of eight binary strings  $\{000, 001, \dots, 111\}$  encompass all possible single-particle states for this example. When the photon is incident on the apparatus, we specify the spatial channel with a subscript; that is, this photon entering through the left spatial channel would be written  $|100\rangle_L$ , and entering through the right would be written  $|100\rangle_R$ .

For the sake of generalization, we use the Greek letter  $\varphi_i$  to stand for a particular single-particle state. The index  $i$  carries information pertaining to the spatial channel. Even indices in  $i$  correspond to  $R$ -channel states, while odd indices in  $i$  correspond to  $L$ -channel states. Furthermore, the states are grouped such that two states

$$\begin{aligned} |\varphi_{2s-1}\rangle &= |\chi_s\rangle_L \\ |\varphi_{2s}\rangle &= |\chi_s\rangle_R \end{aligned} \tag{4.3}$$

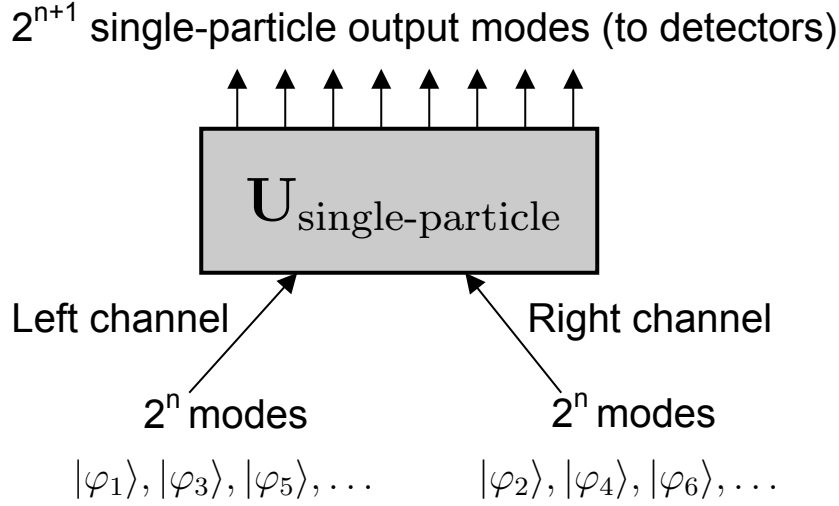


**Figure 4.1** *Schematic of a linear evolution, local measurement device.* A pair of particles enter the measurement apparatus via separate spatial channels (Left and Right). Each particle evolves independently of the other (linear evolution), hence the unitary evolution of single-particle input modes to the set of output modes. Local measurement registers two clicks in the detectors situated at each output mode, projecting the system into a product state of two single-particle output modes (possibly the same mode twice).

are identical except for the choice of *Left* versus *Right* input channel. The value of  $s$  runs from one to  $2^n$ , and the number  $\chi_s$  is simply the binary representation of  $s - 1$ , which is mapped to variable values as discussed above.

The joint-particle, or overall, input states are spanned by the tensor product states  $|\varphi_m\rangle|\varphi_k\rangle$ , with the further restriction that  $m \neq k \pmod{2}$  because we only want to accept states involving one particle in each spatial input channel. In the case of indistinguishable particles, a state written  $|\varphi_m\rangle|\varphi_k\rangle$  carries the implicit (anti-)symmetrization

$$\frac{1}{\sqrt{2}} \left( |\varphi_m\rangle_1 |\varphi_k\rangle_2 \pm |\varphi_k\rangle_1 |\varphi_m\rangle_2 \right) \quad (4.4)$$

for identical particles. The choice of  $+/ -$ , of course, is determined by whether our system obeys bosonic or fermionic particle statistics.

Let us consider some unitary matrix  $\mathbf{U}$ , whose precise definition is based on the details of our measurement apparatus illustrated schematically in

Figure 4.1. We can easily represent a single-particle output state in terms of single-particle input states by applying the unitary evolution embodied in  $\mathbf{U}$ :

$$|i\rangle = \sum_m U_{im} |\varphi_m\rangle \quad (4.5)$$

Because the apparatus is really just a unitary transformation over the single-particle input states, our space of output states  $\{|i\rangle\}$  must likewise have the same  $2^{n+1}$  dimensionality. By convention, the output modes will be labeled by a number between 1 and  $2^{n+1}$ . This makes it easy to refer to them by a detector number, *e.g.*, “Detector 2.”

A complete detection event corresponds to projecting the joint-particle input state onto a particular set of detector states defined by the tensor product  $|i\rangle \otimes |j\rangle$ . As discussed in the context of the input states  $|\varphi_m\rangle |\varphi_k\rangle$ , the detector state  $|i\rangle \otimes |j\rangle$  also carries the implicit (anti-)symmetrization

$$|i\rangle |j\rangle \rightarrow \frac{1}{\sqrt{2}} \left( |i\rangle_1 |j\rangle_2 \pm |j\rangle_1 |i\rangle_2 \right) \quad (4.6)$$

for identical bosons/fermions. Furthermore, because we are restricted to input states with one particle in each spatial channel, a particular detector state must be projected over the subspace of two-particle inputs meeting that criterion. We call this projection the *detection signature*, and denote it  $P_{LR}|i\rangle |j\rangle$ . (The notation  $P_{LR}$  comes from the *Projection* onto states with both *Left* and *Right* channel inputs).

A particular single-detector state can be divided into two separate kets that represent arbitrary superpositions of just *L*-channel or just *R*-channel states:

$$|i\rangle = \alpha_i |l_i\rangle + \beta_i |r_i\rangle \quad (4.7)$$

Here, the ket  $|l_i\rangle$  is some superposition of Left-channel states, and  $|r_i\rangle$  is some superposition of Right-channel states. The subscript  $i$  indicates that these superpositions refer to the  $i^{\text{th}}$  detector state,  $|i\rangle$ .

To illustrate the idea of a detection signature, consider the following example for  $n = 1$ . Let’s define two detector states  $|i\rangle$  and  $|j\rangle$  to be

$$\begin{aligned} |i\rangle &= \frac{1}{\sqrt{2}} (|0\rangle_L - |0\rangle_R) \\ |j\rangle &= \frac{1}{\sqrt{2}} (|1\rangle_L + |1\rangle_R) \end{aligned} \quad (4.8)$$

If we were simply to take the product  $|i\rangle|j\rangle$ , we would get

$$|i\rangle|j\rangle = \frac{1}{2}(|0\rangle_L - |0\rangle_R)(|1\rangle_L + |1\rangle_R) \longrightarrow \quad (4.9)$$

$$= \frac{1}{2} \left[ |0\rangle_L|1\rangle_L + |0\rangle_L|1\rangle_R - |0\rangle_R|1\rangle_L - |0\rangle_R|1\rangle_R \right] \quad (4.10)$$

But, because the space of valid input states does not contain joint-particle kets of the form  $|0\rangle_L|1\rangle_L$  and  $|0\rangle_R|1\rangle_R$  since they represent two particles in the same spatial mode, we want to take the projection  $P_{LR}$  over the subspace of joint-particle input states with one  $L$ -particle state and one  $R$ -particle state. Thus, the *real* detection signature we want to consider is

$$P_{LR}|i\rangle|j\rangle = \frac{1}{\sqrt{2}}(|0\rangle_L|1\rangle_R - |1\rangle_L|0\rangle_R) \quad (4.11)$$

where we must also renormalize the final state. In this example, the Bell state  $|\Psi^-\rangle$  is detected.

Generally speaking, a detection signature  $P_{LR}|i\rangle|j\rangle$  is some superposition of joint-particle input states. These can be translated into the Bell basis by applying the transformation matrix  $\mathbf{M}_n$  from Equation (2.11), and so a given superposition in the detection signature tells us which Bell states are included in that measurement outcome.

### 4.3 Previous Work

It is easily shown that Bell-state measurements using LELM devices are constrained by a simple upper bound to at most  $2^{n+1}$  Bell-state classes; I demonstrate this with a brief argument below. However, previous work has shown that the actual maximum number of distinguishable classes for  $n = 1$  and 2 variables is one less than this simple upper bound, or  $2^{n+1} - 1$  [1; 25; 26]. Philipp Gaebler (HMC '09) showed by construction that one can *always* distinguish  $2^{n+1} - 1$  Bell-state classes using LELM devices [27], but it was not previously known whether the  $2^{n+1}$  upper bound was theoretically achievable for some  $n$ . Such a distinction is important, for example, in determining the maximum channel capacity for quantum dense coding. The proof of a  $2^{n+1} - 1$  bound for  $n = 1$  happens to be algebraically tractable and was first published in 1999 [1]. But the maximum number of distinguishable Bell states for  $n = 2$  was discovered computationally in 2007 after testing all  $\binom{16}{8} = 12,870$  combinations of  $2^{n+1} = 8$  states to show that no such set was distinguishable [25]. A similar computational proof

for  $n = 3$  would involve testing  $\binom{64}{16} \approx 4.9 \times 10^{14}$  cases; clearly the problem becomes a computational nightmare very quickly.

Before I prove the  $2^{n+1} - 1$  maximum in Chapter 5, it will be useful to understand the reasoning behind the  $2^{n+1}$  simple upper bound on Bell-state measurements using LELM devices. The heuristic reason comes from the fact that detecting a single particle does not tell us anything about the entangled joint-particle state in the Bell basis; after all, restricting measurement to a single particle produces randomly distributed outcomes in our basis of choice. Entanglement only manifests itself experimentally upon a *post hoc* comparison between measurements of both particles in the same basis. Furthermore, the maximally-entangled structure of each Bell state ensures that it contains every single-particle state somewhere in its representation. Thus, if a detector can fire at all, it will necessarily have an amplitude to fire on every Bell-state input. The hand-wavy explanation for this comes from the linear evolution constraint, which requires the apparatus to act over the space of *single*-particle inputs. Since the Bell states all contain every single-particle state, each Bell state must in a sense “saturate” the detector space.

It is not immediately obvious, however, that tracing over one of the particles leaves the other in a superposition capable of triggering every detector; after all, couldn’t the apparatus be designed such that the resulting single-particle superposition destructively interferes in some detector mode? To prove this is not the case, we simply realize that the reduced density matrix for either particle of a maximally entangled state leaves an equal-superposition mixture of all single-particle states. Thus, the reduced density matrix is a multiple of the identity, meaning it is basis-independent. Considering  $\rho_{reduced}$  in the detector basis makes it clear that every detector has an amplitude to fire. Detecting a single particle provides no information about the input Bell state.

Because no information can be gleaned from the first detector event, distinguishability must come from one of the  $2^{n+1}$  possibilities for the second detector event. This is the simple upper bound we are looking for; no LELM device can achieve better resolution because there are not enough free parameters in the detection space.

### 4.3.1 Apparatus for maximal distinguishability

This section presents the general structure of a unitary transformation matrix which will reliably distinguish between the maximum  $2^{n+1} - 1$  Bell-state classes for both fermions and bosons. The construction is based on

thesis work done by Philipp Gaebler (HMC '09) [27], but recast in the terminology used for this thesis. I reproduce the argument because it closes the bound on Bell-state distinguishability from below, and illustrates the symmetries in an apparatus capable of maximum distinguishability.

The simplest unitary transformation capable of distinguishing between the maximum  $2^{n+1} - 1$  Bell-state classes for both fermionic and bosonic inputs is given by:

$$\begin{aligned} |2s-1\rangle &= \frac{1}{\sqrt{2}}(|\varphi_{2s-1}\rangle + |\varphi_{2s}\rangle) \\ |2s\rangle &= \frac{1}{\sqrt{2}}(|\varphi_{2s-1}\rangle - |\varphi_{2s}\rangle) \end{aligned} \quad (4.12)$$

for  $s = 1$  to  $2^n$ . This is simply a Hadamard transform between the  $L$  and  $R$  spatial channels for each  $n$ -variable eigenstate  $|\chi_s\rangle$ , and can be achieved quite simply in practice (see Figure 4.2).

For bosons with linear evolution governed by Equation (4.12), detection signatures of the form

$$\begin{aligned} P_{LR}|2s-1\rangle|2s-1\rangle &\longrightarrow |\chi_s\rangle_L|\chi_s\rangle_R \\ P_{LR}|2s\rangle|2s\rangle &\longrightarrow |\chi_s\rangle_L|\chi_s\rangle_R \end{aligned} \quad (4.13)$$

result from the same detector firing twice and pick out the same joint-particle state  $|\chi_s\rangle_L|\chi_s\rangle_R$ . Thus, these detection signatures all identify the class of  $2^n$  hyper-entangled Bell states  $|\Phi^\pm\rangle^{\otimes n}$ . A more detailed discussion on the Bell-basis representation of joint-particle states can be found in Section 6.2. Detection signatures of the form

$$\begin{aligned} P_{LR}|2s\rangle|2s-1\rangle &\longrightarrow 0 \\ P_{LR}|2s-1\rangle|2s\rangle &\longrightarrow 0, \end{aligned} \quad (4.14)$$

on the other hand, are anti-symmetric under particle exchange and do not occur.

For fermions, the roles are reversed; detection signatures  $P_{LR}|2r-1\rangle|2r\rangle$  or  $P_{LR}|2s\rangle|2s-1\rangle$  identify the class of  $2^n$  hyper-entangled Bell states  $|\Phi^\pm\rangle^{\otimes n}$ , while detection signatures  $P_{LR}|2s-1\rangle|2s-1\rangle$  or  $P_{LR}|2s\rangle|2s\rangle$  are symmetric and do not occur.

Any detection signature not of the forms already discussed will give

$$P_{LR}|i\rangle|j\rangle = \frac{1}{\sqrt{2}}(|\chi_r\rangle_L|\chi_s\rangle_R \pm |\chi_s\rangle_L|\chi_r\rangle_R) \quad (4.15)$$

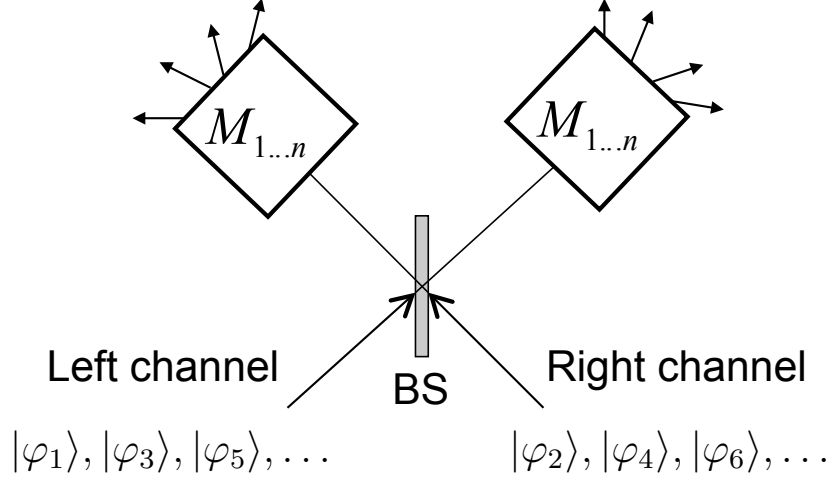


**Figure 4.2** Schematic of an optimal LELM apparatus. Two photons entangled in variables  $1 \dots n$  are incident on a 50/50 beamsplitter, which interferes  $|\varphi_{2s-1}\rangle$  and  $|\varphi_{2s}\rangle$ . Evolution  $M_{1\dots n}$  separates particles by values of the  $n$  variables, so detection is a projective measurement in the  $\{|0\rangle, |1\rangle\}^{\otimes n}$  basis. (If the beamsplitter does not preserve variables  $1 \dots k$ ,  $M_{1\dots k}$  must precede the beamsplitter stage while  $M_{k+1\dots n}$  can follow.) For one-variable Bell states of photon polarization,  $M_{1\dots n}$  is simply  $M_1$  and can be realized with a polarizing beamsplitter. This apparatus embodies the transformation described in Equation 4.12 for photons.

with  $r \neq s$ . Bell states represented by these detection signatures must be tensor products of  $|\Phi^\pm\rangle$  in variables where  $|\chi_r\rangle$  and  $|\chi_s\rangle$  share their eigenvalue, and  $|\Psi^\pm\rangle$  in variables where they do not. Specifying  $\Phi$  vs.  $\Psi$  in each variable narrows the detection signature to a class of at most  $2^n$  Bell states. Furthermore, the sign of the superposition in Equation (4.15) gives the symmetry of the overall state with respect to exchange of  $L$  and  $R$ ; the  $|\Psi^-\rangle$  Bell state was shown in Section 2.4 to be anti-symmetric under this exchange while the others are all symmetric, so a  $+$  ( $-$ ) sign in Equation 4.15 restricts that detection signature to hyper-entangled Bell states with  $|\Psi^-\rangle$  in an even (odd) number of variables to preserve symmetry in the different basis representations. Thus each such detection signature identifies a class of  $2^{n-1}$  Bell states. There are  $2^{n+1} - 2$  classes of this type and one  $|\Phi^\pm\rangle^{\otimes n}$  class, so exactly  $2^{n+1} - 1$  classes are reliably distinguished.

For photons, the optimal apparatus is particularly simple. As shown



in Figure 4.2, a 50/50 beamsplitter performs (up to overall phase shifts) the Hadamard transform of Equation (4.12); the remaining linear evolution separates the input modes according to the value of each variable, so detector clicks perform a projective measurement in the  $\{|0\rangle, |1\rangle\}^{\otimes n}$  basis. Previously determined optimal distinguishability schemes for  $n = 1$  are of this form [1; 26; 28–30].

Unitary transformations not equivalent to Equation (4.12), though they may be more difficult to implement in practice, can also provide distinguishability of the optimal  $2^{n+1} - 1$  classes of Bell states. A modest variation would be to perform Hadamard transforms not just between the left and right channels, but also between the  $|0\rangle$  and  $|1\rangle$  eigenstates for one or more variables; for example, this optimal unitary transformation (for a single variable) is written in the joint-particle unentangled basis of Equation (2.12) as:

$$U_{\text{opt}} = \frac{1}{2} \begin{pmatrix} 1 & 1 & 1 & 1 \\ 1 & -1 & 1 & -1 \\ 1 & 1 & -1 & -1 \\ 1 & -1 & -1 & 1 \end{pmatrix}. \quad (4.16)$$

With polarization-entangled photons, Equation (4.16) is realized by a 50/50 beamsplitter followed by polarizing beamsplitters at  $45^\circ$ . Previous optimal schemes for  $n = 2$  differ further from the ones we describe [25; 31; 32].

### 4.3.2 Use of auxiliary modes

It has been shown that, for projective measurements with linear evolution, distinguishability between input (signal) states cannot be improved by the use of auxiliary modes as long as the signal states are of definite particle number [33; 34]. It is for this reason that we have restricted ourselves to the set of  $2^{n+1}$  orthogonal, single-particle input modes described in Section 4.2, and the unitary evolution constraint guarantees a set of  $2^{n+1}$  orthogonal output (detection) modes.

### 4.3.3 Experimental results

The ease with which hyper-entangled photons are produced in spontaneous parametric downconversion has made it feasible to experimentally implement the various protocols and detection schemes discussed above. For example, photon qubits have been teleported over distances of several kilometers (one such experiment achieved successful teleportation underneath the Danube river!) [35]. Additionally, the Kwiat research group

(among others) has explored the use of so-called “Embedded Bell-state Measurements,” which leverage hyper-entanglement by tracing over a known state in one degree of freedom to achieve complete Bell-state discrimination in the other degree of freedom [31]. Their experimental results show that it is possible to make complete, deterministic Bell-state measurements with LELM devices, so long as we embed the measurement in a higher-dimensional, hyper-entangled state space. This embedded Bell-state measurement process, combined with new a understanding on the limits of LELM devices presented in the next two chapters, suggests promising avenues to further develop techniques of hyper-entangled Bell-state discrimination.

The limit of 3 out of 4 single-variable Bell states distinguishable via LELM has already constrained numerous quantum information experiments [2–4]. Hyper-entanglement between two particles in up to three qubit variables has been demonstrated experimentally [36], and two-variable hyper-entanglement has been used to enable complete resolution of single-variable Bell states, as discussed above. Thus experiments are nearing the threshold of previously-established theoretical bounds on hyper-entangled Bell state distinguishability. The rest of this thesis extends our theoretical understanding of Bell-state measurement to arbitrary degrees of hyper-entanglement, opening the door to experimental exploration with full knowledge of the limitations presented by linear devices.

## Chapter 5

# Proof of maximal distinguishability

### 5.1 Introduction

One might intuitively suspect based on the bounds of Bell-state distinguishability for  $n = 1$  and 2 degrees of freedom (discussed in the previous chapter) that a maximum distinguishability of  $2^{n+1} - 1$  would hold for all  $n$ . But an attempt to build intuition at  $n = 3$  by computational means turned out to be as intractable as one might expect; even after leveraging certain symmetries in the Bell states to reduce the number of cases one must check, it was still too computationally intensive. Instead, we approached this problem from a different angle, looking first at the constraints placed on measurement classes by the maximum Schmidt number permitted under LELM, and then by looking at certain outcomes that are disallowed under exchange symmetries for fermions and bosons. Chapter 6 is dedicated to the approach based on Schmidt number, proving the  $2^{n+1} - 1$  upper bound for disjoint Bell state classes and placing constraints on Bell-state resolution *within* a particular measurement class. This chapter focuses on the more generic proof from exchange symmetries, and applies to situations in which different measurement outcomes might produce overlapping Bell-state classes.

### 5.2 Proof

The  $2^{n+1}$  simple upper bound was obtained in Section 4.3 by realizing that detecting a single particle gives us no information about the possible entan-

gled input states. Because all information in a Bell state resides in the *correlation* between particles rather than in the state of a single particle itself, distinguishability must come from detecting the second particle in conjunction with the first. Previously, we assumed that any of the  $2^{n+1}$  detectors could fire with the second particle. However, I will now show that this is not necessarily the case. Because we must account for the exchange symmetries involved with indistinguishable particles, a joint-detector state that possesses the wrong symmetry will never occur. This phenomenon was illustrated with the optimal scheme presented in Section 4.3.1.

Alternatively, if no such (anti-)symmetric detection signature exists, then I will show that (at least) one detector class must be composed only of Bell states that also appear in other detector classes. Consequently, no set of  $2^{n+1}$  Bell states can be distinguished under LELM, proving the stated  $2^{n+1} - 1$  maximum. This general result, of course, agrees with previous results for  $n = 1$  (3 out of 4) and  $n = 2$  (7 out of 16) [1; 25; 26]. It also demonstrates the only limitation that matters for  $n = 1$ , because the simple upper bound is otherwise large enough to accommodate all Bell states in a single variable. But before I go on to prove this result for indistinguishable particles, I will briefly address the less interesting case of distinguishable particles.

### 5.2.1 Distinguishable Particles

If the particles in the left and right input channels are distinguishable, each output mode  $|i\rangle$  of Equation 4.7 is simply equal to  $|l_i\rangle$  or to  $|r_i\rangle$ . That is, the individual output modes are not superpositions of left- and right-channel inputs because we are capable of distinguishing between them based on which type of particle is detected. Thus,  $2^n$  output modes must be superpositions of the left-channel inputs, and the other  $2^n$  output modes are superpositions of the right-channel inputs. For any detector  $i$ , only  $2^n$  detection signatures  $P_{LR}|i\rangle|j\rangle$  are nonzero. Since all the Bell states must be represented in these  $2^n$  signatures, there are at most  $2^n$  distinguishable classes of Bell states for the case of distinguishable particles.

This result is potentially important for experiments involving indistinguishable particles as well, because experimental convenience might require separate measurement apparatuses for each particle. This is equivalent to the reasoning above, in which we have separated the spatial input modes such that left-channel states trigger a distinct set of  $2^n$  detectors from right-channel states.

### 5.2.2 Indistinguishable Particles

The more interesting case arises with the use of indistinguishable particles, which can exhibit more intricate superpositions. Recall from Chapter 4 that the joint-particle input states  $|\varphi_m\rangle|\varphi_k\rangle$  and joint-detector output states  $|i\rangle|j\rangle$  carry the implicit (anti-)symmetrization

$$\begin{aligned} |\varphi_m\rangle|\varphi_k\rangle &\rightarrow \frac{1}{\sqrt{2}} \left( |\varphi_m\rangle_1 |\varphi_k\rangle_2 \pm |\varphi_k\rangle_1 |\varphi_m\rangle_2 \right) \\ |i\rangle|j\rangle &\rightarrow \frac{1}{\sqrt{2}} \left( |i\rangle_1 |j\rangle_2 \pm |j\rangle_1 |i\rangle_2 \right) \end{aligned} \quad (5.1)$$

where the  $+$  and  $-$  signs hold for bosons and fermions, respectively. Here, the subscripts (1, 2) label the particles, *not* their input channels; remember that the ( $L$ ,  $R$ ) input channel is specified by the parity of  $m$  and  $k$  in the ket  $|\varphi_m\rangle|\varphi_k\rangle$  itself. For fermions, the amplitude to observe two clicks in detector  $|i\rangle$  must always be zero, since  $|i\rangle|i\rangle$  is inherently symmetric. Thus for any detector  $i$ , at most  $2^{n+1} - 1$  detection signatures  $P_{LR}|i\rangle|j\rangle$  are nonzero in fermionic systems. Since all the Bell states are represented in these  $2^{n+1} - 1$  signatures, there are at most  $2^{n+1} - 1$  distinguishable classes of hyper-entangled Bell states for two fermions.

For bosons, consider a single output state  $|i\rangle$  as represented in Equation 4.7. If either coefficient  $\alpha_i$  or  $\beta_i$  is zero, the detection signature  $P_{LR}|i\rangle|i\rangle$  is zero because we lack states from both  $L$  and  $R$  input channels. Thus, there would be at most  $2^{n+1} - 1$  distinguishable classes of Bell states for this trivial case.

If  $|i\rangle$  is a nontrivial superposition  $|i\rangle = \alpha_i|l_i\rangle + \beta_i|r_i\rangle$  of left- and right-channel input states, then some linear combination of output states must satisfy

$$|X\rangle = \sum_j \epsilon_j |j\rangle = \alpha_i |l_i\rangle - \beta_i |r_i\rangle. \quad (5.2)$$

The hypothetical detection signature given by  $P_{LR}|i\rangle|X\rangle$  is zero, because projecting  $|i\rangle|X\rangle$  onto the subspace of joint-particle input states originating in the  $L$  and  $R$  input channels ensures that  $|i\rangle|X\rangle$  is disallowed under exchange. However, this means explicitly that

$$\sum_j \epsilon_j P_{LR}|i\rangle|j\rangle = 0 \quad (5.3)$$

Consider some  $j$  such that  $\epsilon_j \neq 0$ ; any Bell state represented in the detection signature  $P_{LR}|i\rangle|j\rangle$  must also be represented in at least one other detection

signature  $P_{LR}|i\rangle|l\rangle$ , since otherwise Equation (5.3) could never sum to zero in the Bell basis. Thus, it is not possible to reliably distinguish between a class of Bell states that can produce clicks in detectors  $(i, j)$  and a class that can produce clicks in detectors  $(i, l)$ . The number of distinguishable Bell-state classes must therefore be less than the full number of detector signatures involving detector  $i$ , and there can be at most  $2^{n+1} - 1$  distinguishable classes of hyper-Bell states for two bosons.

### 5.2.3 Examples

The discussion in Section 5.2.2 might seem abstract, but let us consider a specific example. Take some first detector state  $|i\rangle$  to be

$$|i\rangle = \frac{1}{2} \left[ |0\rangle_L + |0\rangle_R + |1\rangle_L + |1\rangle_R \right] \quad (5.4)$$

Here,  $\alpha_i|i_i\rangle = \frac{1}{2}(|0\rangle_L + |1\rangle_L)$  and  $\beta_i|r_i\rangle = \frac{1}{2}(|0\rangle_R + |1\rangle_R)$ . There must be some superposition of detectors given by

$$|X\rangle = \sum_j \epsilon_j |j\rangle = \frac{1}{2} \left[ |0\rangle_L + |1\rangle_L - |0\rangle_R - |1\rangle_R \right] \quad (5.5)$$

If we now consider  $|i\rangle|X\rangle$ , we find

$$\begin{aligned} |i\rangle|X\rangle &= \frac{1}{4} \left( |0\rangle_L + |1\rangle_L + |0\rangle_R + |1\rangle_R \right) \left( |0\rangle_L + |1\rangle_L - |0\rangle_R - |1\rangle_R \right) \longrightarrow \\ &P_{LR}|i\rangle|X\rangle = 0 \end{aligned} \quad (5.6)$$

because  $|i\rangle|X\rangle$  is inherently anti-symmetric. If we simply let some detector  $|X\rangle = |j\rangle$ , then  $|i\rangle|j\rangle$  will never fire. Alternatively, if we let  $|X\rangle$  be some non-trivial superposition

$$|X\rangle = \frac{1}{\sqrt{2}}|j\rangle + \frac{1}{\sqrt{2}}|l\rangle \quad (5.7)$$

such that the states  $|j\rangle$  and  $|l\rangle$  are given by

$$\begin{aligned} |j\rangle &= \frac{1}{\sqrt{2}} \left( |0\rangle_L - |0\rangle_R \right) \\ |l\rangle &= \frac{1}{\sqrt{2}} \left( |1\rangle_L - |1\rangle_R \right) \end{aligned} \quad (5.8)$$

then we find that the two detection signatures  $|i\rangle|j\rangle$  and  $|i\rangle|l\rangle$  have identical Bell states:

$$\begin{aligned} |i\rangle|j\rangle &= \frac{1}{2\sqrt{2}} \left( |0\rangle_L + |1\rangle_L + |0\rangle_R + |1\rangle_R \right) \left( |0\rangle_L - |0\rangle_R \right) \longrightarrow \\ P_{LR}|i\rangle|j\rangle &= \frac{1}{\sqrt{2}} \left( |0\rangle_R |1\rangle_R - |1\rangle_L |0\rangle_R \right) \longrightarrow |\Psi^-\rangle \end{aligned} \quad (5.9)$$

and

$$\begin{aligned} |i\rangle|l\rangle &= \frac{1}{2\sqrt{2}} \left( |0\rangle_L + |1\rangle_L + |0\rangle_R + |1\rangle_R \right) \left( |1\rangle_L - |1\rangle_R \right) \longrightarrow \\ P_{LR}|i\rangle|l\rangle &= \frac{1}{\sqrt{2}} \left( |1\rangle_L |0\rangle_R - |0\rangle_R |1\rangle_R \right) \longrightarrow -|\Psi^-\rangle \end{aligned} \quad (5.10)$$

which differ only by a minus sign. Thus, these two detection signatures  $|i\rangle|j\rangle$  and  $|i\rangle|l\rangle$  cannot produce distinguishable sets of Bell states.





## Chapter 6

# Proof of minimum class size

### 6.1 Introduction

In Chapter 5, we demonstrated that LELM devices can produce no more than  $2^{n+1} - 1$  distinguishable classes of Bell states associated with particular measurement outcomes. However, nothing was said about the structure of the individual classes. It might be useful (if it were possible) to “allocate” a measurement class to a single Bell state, such that this measurement outcome achieves a truly unambiguous Bell-state identification when it occurs. It is important to understand whether or not there is a limit to the *size* of Bell-state classes produced under LELM, in addition to their number. This chapter proves a result bounding the best-case resolution that can be achieved within a particular Bell-state class. That is, it shows there is indeed a minimum to the number of Bell states that can be selected in any given LELM detection class.

For clarity, I will state this result in the form of two lemmas, and show briefly how these lemmas reproduce the result of Chapter 5 for disjoint detection classes. I will then prove these lemmas in Section 6.3. I also present an equivalent but alternative proof in Appendix A, which relies more concretely on the rank of certain transformation matrices calculated from our linear evolution operator  $U$ , and the number of Bell states that can be accommodated without exceeding the limits dictated by this matrix rank.

The lemmas defining Bell-state resolution within a particular detection class are as follows:

**Lemma 1.** *If a detector fires twice, we can distinguish a class of no fewer than  $2^n$  states.*

**Lemma 2.** *If two distinct detectors fire, we can distinguish a class of no fewer than  $2^{n-1}$  states.*

Section 6.3 proves these lemmas, but first I will demonstrate how they reproduce the result of Chapter 5 for disjoint classes. To restate the problem, we wish to show there cannot be  $2^{n+1}$  disjoint classes of Bell states distinguishable under LELM. Thus, assume by way of contradiction that there *are* such  $2^{n+1}$  Bell-state classes. Since the detector channels can be relabeled by a simple unitary transformation, without any loss of generality let Detector 1 fire first. The first detector event does not narrow the space of possible Bell states because each Bell state has an amplitude to trigger any single detector (as proved in Section 4.3). Because the first ‘click’ event is meaningless on its own, distinguishability must come from the  $2^{n+1}$  possibilities for the second detector event.

We continue by constructing the optimal (disjoint) partition of our second detector event, according to Lemmas (1) and (2)— $2^n$  Bell states in the class designated by Detector 1 firing again, and  $2^{n-1}$  Bell states in each of the  $2^{n+1} - 1$  classes designated by the other detectors. However, this is

$$2^n(1) + 2^{n-1}(2^{n+1} - 1) = 4^n + 2^{n-1} > 4^n \quad (6.1)$$

states. Since the hyper-entangled state space only includes  $4^n$  Bell states, this partition contradicts the assumption that there can be  $2^{n+1}$  distinguishable classes. Alternatively,  $2^{n+1} - 1$  disjoint classes will neatly partition the states, as  $2^n(1) + 2^{n-1}(2^{n+1} - 2) = 4^n$  states as desired.

Before jumping into the proofs for Lemmas (1) and (2), it is necessary to understand the relationship between superpositions of joint-particle input states (arising from a particular detection signature) and the number of distinct Bell states in that representation. I will discuss this relationship next, and then use it to prove the two lemmas in Section 6.3.

## 6.2 Relationship between Bell states and joint-particle input states

### 6.2.1 Joint-particle input states in the Bell basis

Generically speaking, a detection signature represented in the joint-particle input basis is a superposition of kets taking the form  $|\varphi_m\rangle|\varphi_k\rangle$ . Understanding which states are in the Bell-basis representation of the complete detection signature therefore requires understanding how the joint-particle input states relate individually to the Bell states. Specifically, given some joint-particle input state  $|\varphi_m\rangle|\varphi_k\rangle$ , we want to know which states are in its Bell-basis representation. To prime our intuition, let us first consider the  $n = 1$  case. From the definition of the Bell basis given in Equation (2.7), we easily construct the Bell-basis representation of each joint-particle input state:

$$\begin{aligned} |0\rangle_L|0\rangle_R &= \frac{1}{\sqrt{2}}(|\Phi^+\rangle + |\Phi^-\rangle) \\ |1\rangle_L|1\rangle_R &= \frac{1}{\sqrt{2}}(|\Phi^+\rangle - |\Phi^-\rangle) \\ |0\rangle_L|1\rangle_R &= \frac{1}{\sqrt{2}}(|\Psi^+\rangle + |\Psi^-\rangle) \\ |1\rangle_L|0\rangle_R &= \frac{1}{\sqrt{2}}(|\Psi^+\rangle - |\Psi^-\rangle) \end{aligned} \tag{6.2}$$

The structure of these superpositions should make sense; for joint-particle states that are correlated in the  $|0\rangle/|1\rangle$  basis, we see superpositions of  $\Phi$  Bell states. Similarly, for joint-particle states that are anti-correlated in the  $|0\rangle/|1\rangle$  basis, we see superpositions of  $\Psi$  Bell states.

Extending this to arbitrary  $n$  variables, we see that any given  $n$ -variable, joint-particle input state will have  $2^n$  Bell states in its representation, all coming from the same  $\Phi/\Psi$  class. For example, consider the joint-particle state  $|101\rangle_L|100\rangle_R$ . Based on the discussion in Chapter 2, we see by inspection that this ket has a  $\Phi/\Psi$  signature  $\{\Phi, \Phi, \Psi\}$ . From Equation (6.2) we can decompose this as

$$|101\rangle_L|100\rangle_R \longrightarrow (|1\rangle_L|1\rangle_R)_1 (|0\rangle_L|0\rangle_R)_2 (|1\rangle_L|0\rangle_R)_3 \tag{6.3}$$

$$= \frac{1}{2\sqrt{2}} (|\Phi^+\rangle - |\Phi^-\rangle)_1 (|\Phi^+\rangle + |\Phi^-\rangle)_2 (|\Psi^+\rangle - |\Psi^-\rangle)_3 \tag{6.4}$$

If one were to expand the product in Equation (6.4), it would produce a superposition of  $2^3 = 8$  hyper-entangled Bell states, obtained by selecting one of two Bell states in each term. This superposition is simply the  $\Phi/\Psi$  class  $\{ \Phi, \Phi, \Psi \}$ .

It is easy to see the generalization; each variable contributes two Bell state terms to the product, and so for  $n$  variables there will be  $2^n$  hyper-entangled Bell states in the representation of a single joint-particle input state. Additionally, all of these hyper-entangled Bell states will belong to the same  $\Phi/\Psi$  signature because they are all formed by choosing one of two Bell states from the same class for each of the  $n$  variables. Thus, we conclude that an individual joint-particle input state is a superposition of all  $2^n$  Bell states from the  $\Phi/\Psi$  signature determined by the correlation/anti-correlation properties of that particular state.

From this argument, we also see that joint-particle states associated with *different*  $\Phi/\Psi$  signatures will necessarily have disjoint states in their Bell-basis representation. The proof of this comes from realizing that every hyper-entangled Bell state resulting from a product like the one in Equation (6.4) will differ in single-variable Bell states in the tensor product for variables  $v_s$  where they differ in their  $\Phi/\Psi$  signatures.

As a consequence, we see that only joint-particle states belonging to the *same*  $\Phi/\Psi$  signature have a chance to add destructively in their Bell-basis representations. Superpositions of joint-particle states that belong to different  $\Phi/\Psi$  signatures will necessarily associate a base class of  $2^n$  Bell states for each  $\Phi/\Psi$  signature in the superposition without adding destructively between states of different signatures to reduce the Bell-state class size. Because Lemmas (1) and (2) depend on proving that certain detection events (whose representations are just superpositions of joint-particle kets) cannot represent *fewer* than a given number of Bell states, we want to find ways to minimize the number of states in the Bell-basis representation. Thus, from this point forward we will primarily concern ourselves with superpositions of joint-particle kets belonging to the same  $\Phi/\Psi$  signature, as only these superpositions will lead to a reduction in the Bell-state basis.

### 6.2.2 Single-particle input states and $\Phi/\Psi$ signatures

Because an LELM-constrained apparatus acts on single-particle states (not joint-particle states), it is useful to understand the relationship between  $\Phi/\Psi$  signatures and single-particle kets. In anticipation of arguments to be made proving Lemmas (1) and (2), we will show that two joint-particle states belonging to the same  $\Phi/\Psi$  signature cannot share any  $n$ -variable,

single-particle kets.

To do this, consider two different joint-particle input states  $|\varphi_m\rangle|\varphi_n\rangle$  and  $|\varphi_m\rangle|\varphi_k\rangle$  that share the single-particle ket  $|\varphi_m\rangle$ , and assume by way of contradiction that they both belong to the same  $\Phi/\Psi$  signature  $\zeta$ . Since  $|\varphi_m\rangle|\varphi_n\rangle$  and  $|\varphi_m\rangle|\varphi_k\rangle$  are distinct states,  $|\varphi_n\rangle$  and  $|\varphi_k\rangle$  must differ in one or more variables  $v_s$ . Without loss of generality, suppose  $|\varphi_n\rangle$  and  $|\varphi_k\rangle$  differ in variable  $v_1$ . Then in that variable, the joint ket  $|\varphi_m\rangle|\varphi_n\rangle$  will belong to the opposite Bell-state class as  $|\varphi_m\rangle|\varphi_k\rangle$  and hence cannot have the same  $\Phi/\Psi$  signature  $\zeta$ . This provides the contradiction, proving two states that share a single-particle ket cannot belong to the same  $\Phi/\Psi$  signature. It follows from Section 6.2.1 that superpositions of states directly reducing the size of the Bell-basis representation cannot have kets which share any single-particle states  $|\varphi_m\rangle$ .

### 6.2.3 Bell-state class size and joint-particle superpositions

Finally, it will be necessary to understand how “efficient” a superposition of joint-particle states can be in achieving a reduction in the Bell-state basis. From Section 6.2.1, we see that a single state  $|\varphi_m\rangle|\varphi_k\rangle$  on its own associates a base class of  $2^n$  Bell states with the detection event of interest. However, we will want to know the minimum number of joint-particle states (all within the same  $\Phi/\Psi$  signature) required to reduce the Bell-basis representation of a detection signature to some smaller size  $k \leq 2^n$ . The following argument is a bit abstract (and even uses some abstract algebra!), but a careful reading will make the minimum class-size proof in Section 6.3 clearer.

To understand the minimum number of joint-particle states required to achieve a certain reduction in the Bell-state basis, we introduce a set of symmetry operations on our space of Bell states that invert the  $\pm$  class of the Bell state in a given variable. In other words, the operation  $g_s$  switches  $|\Phi^+\rangle \leftrightarrow |\Phi^-\rangle$  (or  $|\Psi^+\rangle \leftrightarrow |\Psi^-\rangle$ ) in the variable  $v_s$ . These operations  $g_s$  generate a group  $G$  with the structure of  $C_2^{\otimes n}$ . Each element  $g_i \in G$  is its own inverse (and so has order 2), while the whole group  $G$  has order  $2^n$ . Consequently, given any Bell state in our  $\Phi/\Psi$  signature, we can generate all  $2^n$  Bell states in that  $\Phi/\Psi$  signature by applying elements of  $G$ . In the unentangled joint-particle basis, each symmetry operation is equivalent to letting  $\pm|1_s\rangle_L|1_s\rangle_R \rightarrow \mp|1_s\rangle_L|1_s\rangle_R$  for  $\Phi$  states, and  $\pm|1_s\rangle_L|0_s\rangle_R \rightarrow \mp|1_s\rangle_L|0_s\rangle_R$  for  $\Psi$  states (or perhaps more elegantly,  $\pm|1_s\rangle_L \rightarrow \mp|1_s\rangle_L$  in all cases). So while these symmetry operations can change the identity of Bell states in a particular superposition, they do *not* change the identity of

joint-particle kets in the representation. Instead, they simply manipulate the relative phases in the joint-particle basis.

To understand the connection between the number of states present in each basis representation, consider picking  $k$  Bell states which are constructed from some  $r$  joint-particle kets. We may apply the above symmetry operations  $g_i \in G$  without changing the identity of the  $r$  joint-particle states, but in applying all  $2^n$  elements of  $G$  to our superposition we have created  $2^n$  potentially *different* superpositions of  $k$  Bell states each, where all  $2^n$  Bell states from our  $\Phi/\Psi$  signature must appear in at least one of the superpositions on our list. Because the set of superpositions created under the symmetry operations of  $G$  are composed from the same  $r$  (orthogonal) joint-particle kets, the number of linearly independent superpositions in the set tells us the value of  $r$  because both basis representations must have the same dimensionality. In proving Lemmas (1) and (2), we will be interested in the smallest  $r$  required to make a superposition of  $k$  Bell states. This must be bounded by the smallest number of linearly independent superpositions that can be constructed in the Bell basis by applying the symmetry operations of  $G$ . The smallest number will come from a set of superpositions that is maximally disjoint (*i.e.*, has the smallest overlap) but still covers all  $2^n$  Bell states as required. The covering condition requires at least  $2^n/k$  linearly independent superpositions in the Bell basis, and so  $r \geq 2^n/k$ . Notice that for superpositions which represent subgroups  $H \leq G$  and their cosets, the equality holds because the cosets of  $H$  form a partition of  $G$ . By Lagrange's theorem, these superpositions must have  $k = 2^m$  elements because the order of  $H$  must divide  $|G| = 2^n$ . Such superpositions correspond to the most efficient reductions, and are formed by  $r = 2^{n-m}$  states in the joint-particle basis.

#### 6.2.4 Summary

This discussion can be distilled into the following two remarks:

*Remark 1.* If two joint-particle states share the same single-particle ket, they cannot belong to the same  $\Phi/\Psi$  signature. Consequently, a superposition of kets which interfere destructively in the Bell basis must be formed from joint-particle states that cannot be factored in terms of a single input channel.

*Remark 2.* Each  $\Phi/\Psi$  signature that appears in the joint-particle basis representation of a detection signature corresponds to a base class of  $2^n$  Bell states. Reducing the number of Bell states associated with that  $\Phi/\Psi$  signa-

ture to a size  $k \leq 2^n$  requires at least  $2^n/k$  joint-particle kets from the same  $\Phi/\Psi$  signature, where the most efficient reduction comes from Bell-state superpositions corresponding to subgroups (and their cosets) of  $G$ . For these reductions,  $2^m$  joint-particle kets are required to obtain a Bell-state representation of  $2^{n-m}$  states. It is worth noticing that such a reduction can be achieved by working within the tensor product framework of a particular detection signature. That is, by creating a superposition of joint-particle states which can be factored into terms representing each individual variable, the reduction in the Bell-state basis is achieved by forcing some individual terms of this tensor product to be in a superposition that reduces to a single Bell state under the transformation  $\mathbf{M}_0$ . Making such superpositions for  $m$  variables is equivalent to  $2^m$  joint-particle state terms, and  $2^{n-m}$  Bell-state terms.

We will now prove Lemmas 1 and 2.

## 6.3 Proof of minimum Bell-state class size

### 6.3.1 Motivating example

From Section 6.2, we know how a superposition of joint-particle states must be constructed in order to get a small Bell-state class. I will present a few examples to motivate the intuition used in the proof of this section.

Working with  $n = 2$ , consider the simplest case of two detectors,  $|i\rangle$  and  $|j\rangle$ , given by

$$\begin{aligned} |i\rangle &= |00\rangle_L \\ |j\rangle &= |11\rangle_R \end{aligned} \tag{6.5}$$

The detection signature  $P_{LR}|i\rangle|j\rangle$  is then simply

$$|i\rangle|j\rangle = |00\rangle_L |11\rangle_R \tag{6.6}$$

From Section 6.2.1, we know that this solitary joint-particle state  $|00\rangle_L |11\rangle_R$  associates an entire Bell-state class of  $2^n = 4$  states, all with the  $\Phi/\Psi$  signature  $\{\Psi, \Psi\}$ .

Now consider a slightly more complicated case

$$\begin{aligned} |i\rangle &= |00\rangle_L + |00\rangle_R \\ |j\rangle &= |11\rangle_L + |11\rangle_R \end{aligned} \tag{6.7}$$

which has a detection signature  $P_{LR}|i\rangle|j\rangle$  given by

$$P_{LR}|i\rangle|j\rangle = |00\rangle_L|11\rangle_R + |11\rangle_L|00\rangle_R \quad (6.8)$$

Again from Section 6.2.1, we see this is a superposition of two ( $= 2^1$ ) joint-particle kets from the  $\Phi/\Psi$  signature  $\{\Psi, \Psi\}$ , and so only  $2^{n-1} = 2$  Bell states are associated with this detection signature. Specifically, they are the states  $|\Psi^+\rangle \otimes |\Psi^+\rangle$  and  $|\Psi^-\rangle \otimes |\Psi^-\rangle$ .

Can we reduce the Bell-basis representation any further? One might consider making a superposition of more states from the  $\Phi/\Psi$  signature  $\{\Psi, \Psi\}$ . However, to do so requires adding some states to at least one of the detector superpositions  $|i\rangle$  or  $|j\rangle$  given above. But when we go to consider the joint-particle detector state  $|i\rangle|j\rangle$ , any new addition beyond the states given in Equation (6.7) will lead to an additional term in the superposition that also contains one of our single-particle states  $|00\rangle$  or  $|11\rangle$ ; from Section 6.2.2, we know that this new joint-particle state will belong to a different  $\Phi/\Psi$  signature, and so associate a new base class of  $2^n$  Bell states. Instead of achieving the reduction we hoped, it associated another set of  $2^n$  Bell states with that detection signature!

To see this explicitly, consider the following example. Say we wish to select out a single Bell state  $|\Psi^+\rangle \otimes |\Psi^+\rangle$  in a detection class. We can show that

$$|\Psi^+\rangle \otimes |\Psi^+\rangle = |00\rangle_L|11\rangle_R + |01\rangle_L|10\rangle_R + |10\rangle_L|01\rangle_R + |11\rangle_L|00\rangle_R \quad (6.9)$$

and so we need

$$|i\rangle|j\rangle \xrightarrow{?} |00\rangle_L|11\rangle_R + |01\rangle_L|10\rangle_R + |10\rangle_L|01\rangle_R + |11\rangle_L|00\rangle_R \quad (6.10)$$

However, this needs to be factored into a single tensor product between the two detectors. The best attempt we might make is to try factoring it as something like

$$|i\rangle|j\rangle \rightarrow \left(|00\rangle_L + |01\rangle_L + |00\rangle_R + |01\rangle_R\right) \left(|10\rangle_L + |11\rangle_L + |10\rangle_R + |11\rangle_R\right) \quad (6.11)$$

which, when rearranged and projected into a valid detection signature by  $P_{LR}$ , turns into a product with more terms than we anticipated

$$P_{LR}|i\rangle|j\rangle \rightarrow \left(|00\rangle_L + |01\rangle_L\right) \left(|10\rangle_R + |11\rangle_R\right) + \left(|00\rangle_R + |01\rangle_R\right) \left(|10\rangle_L + |11\rangle_L\right) \quad (6.12)$$



Note, I have regrouped terms that will not disappear upon taking the projection  $P_{LR}|i\rangle|j\rangle$ . But the important point is that we now have terms like  $|00\rangle_L|11\rangle_R$  (which we want), as well as terms like  $|00\rangle_L|10\rangle_R$  which share the single-particle state  $|00\rangle_L$ . As a consequence, such terms associate a new  $\Phi/\Psi$  signature and represent an entirely new set of Bell states that do not overlap with the ones we were trying to get rid of. We *were* able to obtain the single state  $|\Psi^+\rangle \otimes |\Psi^+\rangle$ , but at the cost of also getting the state  $|\Psi^+\rangle \otimes |\Phi^+\rangle$ .

For any detection signature describable under LELM, one can always decompose it into terms that look like Equation (6.12), where we separate out a generic joint-particle superposition into two tensor product terms between just  $L$ -channel states and just  $R$ -channel states. This proof by example is rigorously done in [37], which shows that any LELM apparatus cannot achieve a Positive-Operator Value Measure (POVM) with a Schmidt number greater than the number of particles. In our case, we are limited to a Schmidt number no greater than two. The example above illustrates that no matter how we write our two detector states  $|i\rangle$  and  $|j\rangle$ , we will always be able to rearrange the terms into a sum of two tensor product terms between the  $L$ - and  $R$ -channels for a Schmidt number of at most two.

### 6.3.2 Proof of minimum class size

*Proof of Lemma 1.* If the same detector fires twice, we have a detection signature defined by  $|i\rangle|i\rangle$ . Considering now the projection onto the subspace of joint-particle input states with one particle in each spatial channel, we find that

$$|i\rangle|i\rangle = (\alpha_i|l_i\rangle + \beta_i|r_i\rangle)(\alpha_i|l_i\rangle + \beta_i|r_i\rangle) \rightarrow \quad (6.13)$$

$$P_{LR}|i\rangle|i\rangle = |l_i\rangle|r_i\rangle \quad (6.14)$$

which is a single tensor product term and has a Schmidt number of one. If we imagine starting with  $2^n$  Bell states representing an entire  $\Phi/\Psi$  class, the only possibility for reduction comes in creating a superposition of two or more joint-particle states from this  $\Phi/\Psi$  class. However, the joint-particle states in a given  $\Phi/\Psi$  class are in a sense pair-wise entangled; that is, any  $k$ -state subset will have a Schmidt number  $k$ . Because the repeated detector event has a Schmidt number of one, there can be no two-state superposition strictly from the same  $\Phi/\Psi$  class. It would be possible to reduce the Schmidt number to 1 again by allowing a superposition of joint-particle states from multiple  $\Phi/\Psi$  signatures, but this would increase the number

of Bell states by  $2^n$  for each additional  $\Phi/\Psi$  signature appearing in the superposition. To achieve the reduction we are seeking would involve reducing each newly associated  $\Phi/\Psi$  class by more than was possible in a single  $\Phi/\Psi$  class. We quickly see such an approach cannot work, and so this detection signature must have at least  $2^n$  Bell states in its representation.  $\square$

*Proof of Lemma 2.* If two distinct detectors fire, then we have a detection signature defined by  $|i\rangle|j\rangle$ . Again considering the projection onto the subspace of joint-particle input states with one particle in each spatial channel, we get

$$|i\rangle|j\rangle = (\alpha_i|l_i\rangle + \beta_i|r_i\rangle)(\alpha_j|l_j\rangle + \beta_j|r_j\rangle) \rightarrow \quad (6.15)$$

$$P_{LR}|i\rangle|j\rangle = \alpha_i\beta_j|l_i\rangle|r_j\rangle \pm \beta_i\alpha_j|l_j\rangle|r_i\rangle \quad (6.16)$$

This has a Schmidt number of at most two, and so it cannot represent more than two states from the same  $\Phi/\Psi$  signature without associating additional states from other  $\Phi/\Psi$  classes, as discussed above. Specifically, we see that if  $|l_i\rangle|r_j\rangle$  and  $|l_j\rangle|r_i\rangle$  are both from the same  $\Phi/\Psi$  class, we can get a reduction to  $2^{n-1}$  Bell states as described in Section 6.2.3. However, any additional states from that  $\Phi/\Psi$  signature will collaterally associate states from different  $\Phi/\Psi$  signatures. This follows from understanding that superpositions of more than one state in either  $|l_i\rangle$  or  $|r_i\rangle$  will lead to joint-particle states in the final superposition that share single-channel kets, and from Section 6.2.2 we know that every such joint-particle state belongs to a different  $\Phi/\Psi$  class. To achieve any further reduction below  $2^{n-1}$  states would require reducing the newly-associated  $\Phi/\Psi$  classes beyond what was possible with a single class. Again, this approach cannot work, and we are left to conclude that no Bell-state class associated with two distinct detectors firing can have fewer than  $2^{n-1}$  Bell states. This proves Lemma 2.  $\square$

As a final note, the previous optimal schemes published for  $n = 1$  and  $n = 2$  follow this exact class-size structure [1; 25; 26; 28–32]. In particular, they have one large class of  $2^n$  Bell states which is selected when any detector fires twice, and then  $2^{n+1} - 2$  disjoint classes with only  $2^{n-1}$  states in them. Similarly, there are always some detector pairings that do not fire, which represent a detection signature that does not obey the requisite symmetries discussed in Chapter 5.

## Chapter 7

# Conclusion

Chapters 5 and 6 narrow the bounds on distinguishable Bell-state measurements using linear evolution, local measurement devices. Specifically, for hyper-entanglement in  $n$  variables, of the  $4^n$  Bell states one can distinguish at most  $2^{n+1} - 1$  classes. Distinguishability also comes in a structured manner. A certain measurement outcome is indicated by “clicks” in two detectors. If the same detector fires twice (only possible for bosonic systems), then the result of that measurement is a Bell-state class of *no fewer than*  $2^n$  hyper-entangled Bell states. If two distinct detectors fire, the result is a Bell-state class of *no fewer than*  $2^{n-1}$  hyper-entangled Bell states. These results reproduce published results and proposed experimental setups for  $n = 1$  and  $2$ . Furthermore, Philipp Gaebler (HMC '09) showed that it is always possible to distinguish  $2^{n+1} - 1$  Bell state classes, and so the bounds on distinguishability have been closed from both ends.

This thesis also casts the discussion of Bell-state distinguishability in a new light, considering fundamental symmetries in the detection process with LELM devices. Approaching the problem from an appeal to symmetry helps us to better understand the algorithmic proofs of the same numerical result for  $n = 1$  and  $n = 2$ . It also helps to intuitively clarify why we cannot distinguish between all 4 Bell states at  $n = 1$ , as we might expect from the simple upper bound on linear evolution, local measurement.

The types of symmetries that occur in these detection outcomes imply that for every first detector event, there is either one second detector event that is disallowed under the relevant particle statistics, or pairs of second detector events which have identical Bell states.

Future directions for this research might include looking at hyper-entangled qu-trits (entangled three-level systems), or hyper-entangled qu-dits (entan-

gled  $d$ -level systems) more generally. One might also pursue bounds on distinguishability for non-maximally entangled states, or ask how many copies of a hyper-entangled Bell state are required to unambiguously identify it. Regardless, knowing the precise limitations of LELM measurements in the Bell basis will guide future experimental work in quantum communication and in quantum information science more generally.

## Appendix A

# Alternate minimum class-size proof

This appendix shows an alternative argument for the minimum class-size presented in Chapter 6. It stems from the work I did last summer, and uses slightly different notation from that used in the rest of this thesis. However, there are many common notational threads, and it should not be difficult to pick up after reading Chapters 2 and 4. Section A.1 explains the notational changes, and then the alternative proof itself appears in Section A.2. There is also some overlap in the background argument relating the joint-particle states to the Bell basis, but I chose to still include those sections for the sake of coherence.

### A.1 Notation and representations of Bell/detector states

It is useful to think of the two-particle states in terms of an entangled Bell basis, an unentangled basis of two-particle states, *and* a basis of single-particle states underlying the two-particle state space. Throughout this paper, we will adopt the following notational convention: kets that are tensor products of all  $n$ -variable states will be designated by Greek letters, and kets that just contain the state of a single variable will be designated by Roman letters. Joint-particle kets refer to the product of two single-particle states (*i.e.*, the product of the L and R spatial channels). Thus,  $|x\rangle_s = |v_L v_R\rangle_s$  is the joint-particle input ket composed of both L and R spatial channels for a single variable  $v_s$ , whereas the joint-particle ket  $|\varphi_i\rangle|\varphi_j\rangle$  is the product of both L and R single-particle states which each specify all  $n$  variables for the system. The joint-particle states define an unentangled basis for the two-

particle system, but in any two-state variable we can equivalently use the Bell basis, which consists of the four maximally-entangled states given by

$$|\Phi^\pm\rangle = \frac{1}{\sqrt{2}} \left( |0\rangle_L |0\rangle_R \pm |1\rangle_L |1\rangle_R \right) \quad (\text{A.1})$$

$$|\Psi^\pm\rangle = \frac{1}{\sqrt{2}} \left( |0\rangle_L |1\rangle_R \pm |1\rangle_L |0\rangle_R \right) \quad (\text{A.2})$$

The Bell states (A.1) and (A.2) are easily represented by a unitary transformation matrix  $\mathbf{M}_0$ , which transforms a state from the unentangled joint-particle input basis to the entangled Bell basis

$$\begin{pmatrix} |\Phi^+\rangle \\ |\Phi^-\rangle \\ |\Psi^+\rangle \\ |\Psi^-\rangle \end{pmatrix} = \mathbf{M}_0 \begin{pmatrix} |0_L 0_R\rangle \\ |1_L 1_R\rangle \\ |0_L 1_R\rangle \\ |1_L 0_R\rangle \end{pmatrix}, \quad \mathbf{M}_0 = \frac{1}{\sqrt{2}} \begin{pmatrix} 1 & 1 & 0 & 0 \\ 1 & -1 & 0 & 0 \\ 0 & 0 & 1 & 1 \\ 0 & 0 & 1 & -1 \end{pmatrix} \quad (\text{A.3})$$

For entanglement in  $n$  variables, the complete state is a tensor product of Bell states for each degree of freedom. Thus the larger Hilbert space of complete states has dimension  $4^n$ , and the transformation from the joint-channel input basis to the Bell basis is represented by a  $4^n \times 4^n$  matrix  $\mathbf{M} = \mathbf{M}_0^{\otimes n}$ .

Consider some apparatus constrained by LELM, where each detection channel is expressed as a superposition of single-particle input states  $|\varphi_i\rangle$  (which, recall, specify all  $n$  variables for the system in addition to the spatial channel). In general, some detector mode

$$|\alpha\rangle = \sum_{i=1}^{2^{n+1}} a_i |\varphi_i\rangle \quad (\text{A.4})$$

is written as an arbitrary superposition of all single-particle input states  $|\varphi_i\rangle$ . Here, even indices in  $|\varphi_i\rangle$  are given to right channel states, and odd indices are given to left channel states. A detection signature composed of two ‘click’ events (because there are two particles) realizes a Positive Operator Valued Measurement (POVM) [14] and is characterized by

$$|\alpha\rangle|\beta\rangle = \sum_{i=1}^{2^{n+1}} \sum_{j=1}^{2^{n+1}} a_i b_j |\varphi_i\rangle |\varphi_j\rangle \quad (\text{A.5})$$

The detection signature  $|\alpha\rangle|\beta\rangle$  in Equation A.5 is expressed in the unentangled joint-particle basis  $\{|\varphi_i\rangle|\varphi_j\rangle\}$ , where we must additionally impose the condition

$$a_i b_j = 0 \text{ for } i \equiv j \pmod{2} \quad (\text{A.6})$$

because our space of joint-particle input states does not include any kets in which both particles belong to the same spatial channel. However, the form of (A.5) is convenient because we can easily transform the state into the Bell basis via the matrix  $\mathbf{M}$ . This makes it easy to understand which Bell states have an amplitude to trigger a given detection event based on their presence in its representation, and hence which Bell states are indistinguishable under that detection outcome.

It will be useful in our line of reasoning to express the coefficients  $a_i b_j$  in a matrix  $\boldsymbol{\theta}$ , where

$$\tau_{ij} = a_i b_j \quad (\text{A.7})$$

and of course Condition A.6 still holds. Because our particles are identical, the physically significant state is not  $|\varphi_i\rangle|\varphi_j\rangle$ , but instead the properly symmetrized version  $\frac{1}{\sqrt{2}}(|\varphi_i\rangle|\varphi_j\rangle \pm |\varphi_j\rangle|\varphi_i\rangle)$  where the sign is chosen based on whether the system obeys bosonic or fermionic particle statistics. This is reflected in our notation by the matrix  $\mathbf{T}$ , where

$$\mathbf{T} = \frac{1}{\sqrt{2}}(\tau \pm \tau^T) \quad (\text{A.8})$$

Consequently, the entry  $T_{ij} = \frac{1}{\sqrt{2}}(a_i b_j \pm a_j b_i)$  is the amplitude that our system existed in a given joint-particle state  $|\varphi_i\rangle|\varphi_j\rangle$  when detectors  $(\alpha, \beta)$  are triggered.

## A.2 Proof of no-go theorem for general $n$

Let us begin with two lemmas which, if true, impose a maximum of  $2^{n+1} - 1$  disjoint classes of Bell states:

**Lemma 3.** *If a detector fires twice, we can distinguish a class of no fewer than  $2^n$  states.*

**Lemma 4.** *If two distinct detectors fire, we can distinguish a class of no fewer than  $2^{n-1}$  states.*

Proving these lemmas will prove the maximum number of disjoint classes by a simple counting argument: assume by way of contradiction that there are  $2^{n+1}$  classes distinguishable under LELM. Since the detector channels can be relabeled by a simple unitary transformation, without any loss of generality let Detector 1 fires first. The first detector event does not narrow the space of possible Bell states because each Bell state has an amplitude

to trigger any single detector. This results from the fact that every single-particle input state appears somewhere in the representation of each Bell state, and thus the space of single-detector outcomes is completely covered by each of the Bell states. Because the first ‘click’ event is meaningless on its own, distinguishability must come from the  $2^{n+1}$  possibilities for the second detector event.

We continue by constructing the optimal (disjoint) partition of our second detector event— $2^n$  Bell states in the class designated by Detector 1 firing again, and  $2^{n-1}$  Bell states in each of the  $2^{n+1} - 1$  classes designated by the other detectors. However, this is  $2^n(1) + 2^{n-1}(2^{n+1} - 1) = 4^n + 2^{n-1} > 4^n$  states. Since our space only includes  $4^n$  Bell states, this partition contradicts the assumption that there are  $2^{n+1}$  distinguishable classes. Alternatively,  $2^{n+1} - 1$  disjoint classes can partition the states, as  $2^n(1) + 2^{n-1}(2^{n+1} - 2) = 4^n$  states as desired. We will prove Lemmas 3 and 4 in Section A.2.2, but first we need to understand the relationship between superpositions of joint-particle input states (arising from a particular detection event) and the number of distinct Bell states in their representation.

*Temporary note to the reader 1.* OK, i’m worried again... why do the classes have to be disjoint? I could imagine a situation in which we have  $2^{n+1}$  orthogonal classes, where there are  $2^{n+1} - 1$  classes of  $2^{n-1}$  states each, and one class of  $2^n$  states which overlaps with some of the other classes. Is our argument really just that any LELM apparatus cannot define a class of fewer than  $2^{n-1}$  (or  $2^n$ ) states with a single detection outcome? Isn’t this really the important argument anyways?

### A.2.1 Relationship between Bell states and input/detection channels

Given some joint-particle input state  $|\varphi_i\rangle|\varphi_j\rangle$ , we wish to know which states are in its Bell-basis representation. From the transformation in Equation A.3, we see that depending on the state of  $|\varphi_i\rangle|\varphi_j\rangle$  in each variable  $v_s$ , we can determine which Bell states will be non-zero in that variable after the change of basis. Specifically, if  $v_s$  has the *same* value for both L and R spatial channels (*i.e.*, either  $|0\rangle_L|0\rangle_R$  or  $|1\rangle_L|1\rangle_R$ ), then the Bell-basis representation of that variable will be a superposition of both  $\Phi^+$  and  $\Phi^-$  states. Similarly, if  $v_s$  possesses *opposite* values in the L and R channels (*i.e.*, either  $|0\rangle_L|1\rangle_R$  or  $|1\rangle_L|0\rangle_R$ ), then the Bell-basis representation will be a superposition of  $\Psi^+$  and  $\Psi^-$  states. From this, we see that a single joint-particle ket with  $n$  variables must have  $2^n$  states in its Bell-basis representation, since each variable contributes two terms to the Bell-basis tensor product. The classifica-



tion of  $|\varphi_i\rangle|\varphi_j\rangle$  as belonging to a “ $\Phi$ ” or “ $\Psi$ ” class for each variable defines the state’s  $\Phi/\Psi$  signature. We can see that two states  $|\varphi_i\rangle|\varphi_j\rangle$  and  $|\varphi_k\rangle|\varphi_l\rangle$  which belong to the same  $\Phi/\Psi$  signature will have identical Bell states in their representations (although the relative phases will be different). However, two states which belong to *different*  $\Phi/\Psi$  signatures will necessarily have disjoint Bell states in their representations, as they will always have a different Bell state in the tensor product for variables  $v_s$  where they differ in their  $\Phi/\Psi$  signatures. Therefore, superpositions of joint-particle kets that belong to the same  $\Phi/\Psi$  signature have the chance to add destructively in their Bell-basis representation, whereas the disjoint nature of states belonging to different  $\Phi/\Psi$  signatures will require that they always add to increase the number of states in the Bell basis. Lemmas 3 and 4 depend on proving that certain detection events (whose representations are just superpositions of joint-particle kets) cannot represent *fewer* than a given number of Bell states, and so we want to find ways to minimize the number of states in the Bell-basis representation. Thus, from this point forward we will only concern ourselves with superpositions of joint-particle kets belonging to the same  $\Phi/\Psi$  signature, as only these will produce a reduction in the Bell-state basis.

Because an LELM-constrained apparatus acts on single-particle states (not joint-particle states), it is useful to understand the idea of a  $\Phi/\Psi$  signature in terms of single-particle kets. In anticipation of arguments to be made in proving Lemmas 3 and 4, we will show that two joint-particle states belonging to the same  $\Phi/\Psi$  signature cannot share any  $n$ -variable single-particle kets. To do this, consider some superposition of two different joint-particle input states  $|\varphi_i\rangle|\varphi_j\rangle$  and  $|\varphi_i\rangle|\varphi_k\rangle$  that share the single-particle ket  $|\varphi_i\rangle$ , and assume by way of contradiction that they both belong to the same  $\Phi/\Psi$  signature  $\zeta$ . Since  $|\varphi_i\rangle|\varphi_j\rangle$  and  $|\varphi_i\rangle|\varphi_k\rangle$  are distinct states,  $|\varphi_j\rangle$  and  $|\varphi_k\rangle$  must differ in one or more variables  $v_s$ . Without loss of generality, suppose  $|\varphi_j\rangle$  and  $|\varphi_k\rangle$  differ in variable  $v_1$ . Then in that variable, the joint ket  $|\varphi_i\rangle|\varphi_k\rangle$  will belong to the opposite  $\Phi/\Psi$  class as  $|\varphi_i\rangle|\varphi_j\rangle$  and hence cannot have the same  $\Phi/\Psi$  signature  $\zeta$ . This provides the contradiction, proving two states that share a single-particle ket cannot belong to the same  $\Phi/\Psi$  signature. It follows that superpositions of states directly reducing the size of the Bell-basis representation cannot have kets which share any single-particle states  $|\varphi_i\rangle$ .

Finally, it will also be necessary to understand how “efficient” a superposition of joint-particle states can be in achieving a reduction in the Bell-state basis. Clearly, a single state  $|\varphi_i\rangle|\varphi_j\rangle$  on its own associates a base class of  $2^n$  Bell states to the detection event of interest. However, we will

want to know the minimum number of joint-particle states (all within the same  $\Phi/\Psi$  signature) required to reduce the Bell-basis representation of a detection event to some smaller size  $k \leq 2^n$ . To do so, we introduce a set of symmetry operations on our space of Bell states that invert the  $\pm$  class of the Bell state in a given variable. In other words, the operation  $g_s$  switches  $\Phi^+ \leftrightarrow \Phi^-$  (or  $\Psi^+ \leftrightarrow \Psi^-$ ) in the variable  $v_s$ . These operations  $g_s$  generate a group  $G$  with the structure of  $C_2^{\otimes n}$ . Each element  $g_i \in G$  is its own inverse (and so has order 2), while the whole group  $G$  has order  $2^n$ . Consequently, given any Bell state in our  $\Phi/\Psi$  signature, we can generate all  $2^n$  Bell states in that  $\Phi/\Psi$  signature by applying each element of  $G$ . In the unentangled joint-particle basis, each symmetry operation is equivalent to letting  $\pm|1_L 1_R\rangle_s \rightarrow \mp|1_L 1_R\rangle_s$  for  $\Phi$  states, and  $\pm|1_L 0_R\rangle_s \rightarrow \mp|1_L 0_R\rangle_s$  for  $\Psi$  states (or perhaps more simply put,  $\pm|1_L\rangle \rightarrow \mp|1_L\rangle$ ). So while these symmetry operations can change the identity of Bell states in a particular superposition, they do *not* change the identity of joint-particle kets in the representation. Instead, they simply manipulate the relative phases in the joint-particle basis.

To understand the connection between the number of states present in each basis representation, consider picking  $k$  Bell states which are constructed from some  $r$  joint-particle kets. We may apply the above symmetry operations  $g_i \in G$  without changing the identity of the  $r$  joint-particle states, but in applying all  $2^n$  elements of  $G$  to our superposition we have created  $2^n$  potentially *different* superpositions of  $k$  Bell states each, where all  $2^n$  Bell states from our  $\Phi/\Psi$  signature must appear in at least one of the superpositions on our list. Because the set of superpositions created under the symmetry operations of  $G$  are composed of the same  $r$  (orthogonal) joint-particle kets, the number of linearly independent superpositions in the set tells us the value of  $r$  because both basis representations must have the same dimensionality. In proving Lemmas 3 and 4, we will be interested in the smallest  $r$  required to make a superposition of  $k$  Bell states. This must be bounded by the smallest possible number of linearly independent superpositions that can be constructed by applying the symmetry operations of  $G$ . This smallest number of such superpositions will come from a set that is maximally disjoint (*i.e.*, has the smallest overlap) but still covers all  $2^n$  Bell states. This requires at least  $2^n/k$  linearly independent superpositions, and so  $r \geq 2^n/k$ . Notice that for superpositions which represent subgroups  $H \leq G$  and their cosets, the equality holds because the cosets of  $H$  form a partition of  $G$ . By Lagrange's theorem, these superpositions must have  $k = 2^m$  elements because the order of  $H$  must divide  $|G| = 2^n$ . Such superpositions correspond to the most efficient reductions.

The discussion above can be distilled into the following remarks:

*Remark 3.* If two joint-channel kets share the same single-channel ket, they cannot belong to the same  $\Phi/\Psi$  signature. Hence, a superposition which reduces the number of states in the Bell basis must be formed from joint channel kets of the form  $|\varphi_i\rangle|\varphi_j\rangle, |\varphi_k\rangle|\varphi_m\rangle$ , etc. where  $i \neq j \neq k \neq m \neq \dots$

*Remark 4.* Each  $\Phi/\Psi$  signature in the superposition of a detection event corresponds to a base class of  $2^n$  Bell states. Reducing the number of Bell states associated with that  $\Phi/\Psi$  signature to a size  $k \leq 2^n$  requires at least  $2^n/k$  joint-particle kets from the same  $\Phi/\Psi$  signature, where the most efficient reduction comes from Bell-state superpositions corresponding to subgroups (and their cosets) of  $G$ . For these reductions,  $2^m$  joint-particle kets are required to obtain a Bell-state representation of  $2^{n-m}$  states. It is worth noticing that such a reduction can be achieved by working within the tensor product framework. That is, by creating a superposition of joint-particle states which can be factored into terms representing each variable, one can make two-term superpositions in individual variables which reduce to a single Bell state under the transformation  $\mathbf{M}$ . Making such superpositions for  $m$  variables is equivalent to  $2^m$  joint-particle state terms and  $2^{n-m}$  Bell-state terms. We will now prove Lemmas 3 and 4.

### A.2.2 Proofs for Lemmas 1 and 2

*Lemma 3.* If the same detector fires twice, we require that  $|\alpha\rangle = |\beta\rangle$  and so in Equation A.5  $a_i = b_i$  forcing  $\tau$  from (A.7) to be symmetric. For bosonic systems, this means  $\mathbf{T} = \sqrt{2}\tau$ , while in fermionic systems we get  $\mathbf{T} = \mathbf{0}$ . This makes sense, because two half-integral spin particles cannot both end up in the same detection mode. Exploring the bosonic case, our construction of  $\tau$  implies  $\mathbf{T}$  must have rank 2. This is easily shown by noticing that Condition A.6 forces Column 1 to have zeros in rows with odd indices and Column 2 to have zeros in rows with even indices, meaning these columns have strictly non-overlapping non-zero entries and so are linearly independent. However, every other column  $j$  differs from one of these first two columns by a multiplicative constant ( $b_j/b_1$  for odd columns and  $b_j/b_2$  for even columns) and therefore they do not form additional linearly independent columns. Thus, there are only two linearly independent columns in  $\mathbf{T}$ , making it rank 2.

Now consider how we might impose criteria for the detection signature  $|\alpha\rangle|\alpha\rangle$  by setting certain entries in  $\mathbf{T}$  to be non-zero, which corresponds to particular joint-particle states having non-zero amplitude in the represen-

tation of the detection event. In doing so, we must not violate the rank 2 nature of  $\mathbf{T}$  and hence are constrained to criteria in which  $\mathbf{T}$  has no more than two linearly independent columns. We wish to show that no such criteria can define a class of fewer than  $2^n$  Bell states.

As discussed above, a single joint-particle ket  $|\varphi_i\rangle|\varphi_j\rangle$  initially associates a base class of  $2^n$  Bell states to the detection event  $|\alpha\rangle|\alpha\rangle$ . If we consider the entries in  $\mathbf{T}$  corresponding to this state, we must make  $T_{ij} = T_{ji} \neq 0$ . Since  $i$  and  $j$  have opposite parity, this already defines two linearly independent columns in  $\mathbf{T}$ . For the sake of argument, however, let us consider introducing additional kets (from the same  $\Phi/\Psi$  signature) to reduce the size of the associated Bell-state class. From Section A.2.1, we know that it requires at least  $2^n/k$  joint-particle kets to obtain  $k \leq 2^n$  Bell states. For  $k = 2^n$ , this is just the single state  $|\varphi_i\rangle|\varphi_j\rangle$ , but for  $k < 2^n$  we must introduce *additional* joint-particle states from the same  $\Phi/\Psi$  signature.

As we introduce these additional states, we must make the corresponding changes to entries in  $\mathbf{T}$  to reflect these additional kets in the superposition. However, the changes may not introduce additional linearly independent columns. Consider some number  $r = \lceil 2^n/k \rceil$  joint-channel kets, which are equivalent to  $k$  states in the Bell basis. These  $r$  kets must be of the form  $|\varphi_i\rangle|\varphi_j\rangle$ ,  $|\varphi_k\rangle|\varphi_l\rangle$ , etc. where  $i \neq j \neq k \neq l \dots$  because they all belong to the same  $\Phi/\Psi$  signature. If we simply make the corresponding entries in  $\mathbf{T}$  non-zero, they will necessarily define  $2 \cdot r$  linearly independent columns. Thus, for  $r > 1$  we must somehow modify other entries of  $\mathbf{T}$  to preserve the rank 2 nature of the matrix. Consider two columns  $i$  and  $j$  corresponding to the single joint-particle ket  $|\varphi_i\rangle|\varphi_j\rangle$ . These *must* be linearly independent from Condition A.6, and so without loss of generality we consider ways in which the other  $2 \cdot (r - 1)$  columns can be brought into linear dependence with these two. Each additional ket  $|\varphi_k\rangle|\varphi_l\rangle$  we introduce forces  $T_{kl} = T_{lk} \neq 0$  and creates two more linearly independent columns  $k$  and  $l$ . Thus, at a bare minimum we must make the entries in rows  $l$  and  $k$  of columns  $i$  and  $j$  non-zero, that is,  $T_{kj} \neq 0$  and  $T_{li} \neq 0$ . But this introduces two new kets,  $|\varphi_k\rangle|\varphi_j\rangle$  and  $|\varphi_i\rangle|\varphi_l\rangle$ , which cannot belong to the same  $\Phi/\Psi$  signature as our original ket  $|\varphi_i\rangle|\varphi_j\rangle$  because they both share a single-particle state with that ket. Similarly, each joint-particle state we introduce to the superposition will require (at a minimum) modifying entries in rows of  $i$  and  $j$  to maintain the rank-2 nature of  $\mathbf{T}$ , which necessarily introduces at least one more  $\Phi/\Psi$  signature. Thus,  $r$  joint-particle kets implies (at least)  $r$   $\Phi/\Psi$  signatures, which could at most be reduced to  $k$  states (because by symmetry, reducing further would require introducing new  $\Phi/\Psi$  signatures). From this, we see that there are at least  $k \cdot r = k \cdot 2^n/k = 2^n$  Bell

states, regardless of how hard we try to reduce the size of this class. This proves Lemma 3.  $\square$

*Lemma 4.* In the case where  $|\alpha\rangle$  and  $|\beta\rangle$  represent separate detectors, we no longer require that  $a_i = b_i$  and so retain the full expression  $\mathbf{T} = \frac{1}{\sqrt{2}}(\tau \pm \tau^T)$  from (A.8). As shown in the proof of Lemma 3,  $\tau$  is rank 2 and so it follows trivially that  $\text{Rank}(\mathbf{T}) \leq 4$ . This means there can be at most four linearly independent columns in  $\mathbf{T}$ , a fact which constrains the criteria we may impose in defining the detection event  $|\alpha\rangle|\beta\rangle$ . We will prove that no set of criteria for  $|\alpha\rangle|\beta\rangle$  can produce an associated class of fewer than  $2^{n-1}$  Bell states.

Consider  $k$  Bell states designated by  $r \geq 2^n/k$  joint-particle kets from the same  $\Phi/\Psi$  signature  $\zeta$ , which are non-zero in  $|\alpha\rangle|\beta\rangle$ . Each of these kets  $|\varphi_i\rangle|\varphi_j\rangle, |\varphi_k\rangle|\varphi_l\rangle, |\varphi_o\rangle|\varphi_p\rangle, \dots$  are specified by sets of two linearly independent columns in  $\mathbf{T}$ . If no further modifications are made to  $\mathbf{T}$ , these columns will all be linearly independent from each other as well, because  $i \neq j \neq k \neq l \dots$ . We know that  $\mathbf{T}$  has at most four linearly independent columns, so without loss of generality we can choose two pairs of columns  $i, j$  and  $k, l$  to be linearly independent from each other (where  $i, j$  and  $k, l$  have opposite parity because they must correspond to valid kets in our joint-particle input space). As we accommodate the  $r$  joint-particle kets in  $\zeta$ , we must bring the corresponding  $2 \cdot r$  columns into linear dependence with one of  $i$  through  $l$ . By the pigeonhole principle, one column must have at least  $2 \cdot r/4 = r/2$  entries. Each of these entries will correspond to joint-particle states which all share a single-channel ket (because the entries in  $\mathbf{T}$  lie in the same column) and so will define  $r/2$  different  $\Phi/\Psi$  signatures. Thus, we require at least  $r/2$   $\Phi/\Psi$  signatures, which could in turn be reduced to no fewer than  $k$  Bell states (because again, reducing any of them further would require introducing more  $\Phi/\Psi$  signatures). We once more arrive at a zero-sum game, because this defines at least  $k \cdot r/2 = k \cdot 2^n/(2k) = 2^{n-1}$  Bell states. Hence, any effort to reduce the size of the Bell state representation cannot achieve classes smaller than  $2^{n-1}$  Bell states, as desired. This proves Lemma 4.

The proof of Lemmas 3 and 4 is sufficient to prove our statement, that it is impossible to distinguish between more than  $2^{n+1} - 1$  disjoint classes of Bell states under linear evolution and local measurement.  $\square$



# Bibliography

- [1] N. Lütkenhaus, J. Calsamiglia, and K.-A. Suominen. Bell measurements for teleportation. *Phys. Rev. A*, 59(5):3295–3300, May 1999.
- [2] Jian-Wei Pan, Dik Bouwmeester, Harald Weinfurter, and Anton Zeilinger. Experimental entanglement swapping: Entangling photons that never interacted. *Phys. Rev. Lett.*, 80(18):3891–3894, May 1998.
- [3] Klaus Mattle, Harald Weinfurter, Paul G. Kwiat, and Anton Zeilinger. Dense coding in experimental quantum communication. *Phys. Rev. Lett.*, 76(25):4656–4659, Jun 1996.
- [4] Dik Bouwmeester, Jian-Wei Pan, Klaus Mattle, Manfred Eibl, Harald Weinfurter, and Anton Zeilinger. Experimental quantum teleportation. *Nature*, 390(6660):575–579, Dec 1997.
- [5] Charles H. Bennett, Gilles Brassard, Claude Crépeau, Richard Jozsa, Asher Peres, and William K. Wootters. Teleporting an unknown quantum state via dual classical and einstein-podolsky-rosen channels. *Phys. Rev. Lett.*, 70(13):1895–1899, Mar 1993.
- [6] Tzu-Chieh Wei, Julio T. Barreiro, and Paul G. Kwiat. Hyperentangled bell-state analysis. *Phys. Rev. A*, 75(6):060305, Jun 2007.
- [7] A Einstein, B Podolsky, and N Rosen. Can quantum-mechanical description of physical reality be considered complete? *Physical Review*, 41(777), May 1935.
- [8] J.S. Bell. On the einstein podolsky rosen paradox. *Physics*, 1(3):195, 1964.
- [9] John F. Clauser, Michael A. Horne, Abner Shimony, and Richard A. Holt. Proposed experiment to test local hidden-variable theories. *Phys. Rev. Lett.*, 23(15):880–884, Oct 1969.

- [10] Alain Aspect, Philippe Grangier, and Gérard Roger. Experimental tests of realistic local theories via bell's theorem. *Phys. Rev. Lett.*, 47(7):460–463, Aug 1981.
- [11] Alain Aspect, Philippe Grangier, and Gérard Roger. Experimental realization of einstein-podolsky-rosen-bohm gedankenexperiment: A new violation of bell's inequalities. *Phys. Rev. Lett.*, 49(2):91–94, Jul 1982.
- [12] Alain Aspect, Jean Dalibard, and Gérard Roger. Experimental test of bell's inequalities using time- varying analyzers. *Phys. Rev. Lett.*, 49(25):1804–1807, Dec 1982.
- [13] J. Altepeter, E. Jeffrey, and P. Kwiat. Phase-compensated ultra-bright source of entangled photons. *Opt. Express*, 13(22):8951–8959, Oct 2005.
- [14] John Preskill. Notes for quantum computation (physics 219). <http://www.theory.caltech.edu/people/preskill/ph229/>, May 2011.
- [15] Paul G. Kwiat. Hyper-entangled states. *Journal of Modern Optics*, 44(11):2173–2184, 1997.
- [16] Paul G. Kwiat, Edo Waks, Andrew G. White, Ian Appelbaum, and Philippe H. Eberhard. Ultrabright source of polarization-entangled photons. *Phys. Rev. A*, 60(2):R773–R776, Aug 1999.
- [17] John S. Townsend. *A Modern Approach to Quantum Mechanics*. University Science Books, 2000.
- [18] Teleportation. <http://www.oed.com/view/Entry/198734>, May 2011.
- [19] W.K. Wootters and W.H. Zurek. A single quantum cannot be cloned. *Nature*, 299:802–803, October 1982.
- [20] D. Dieks. Communication by epr devices. *Physics Letters A*, 92(6):271 – 272, 1982.
- [21] M. Żukowski, A. Zeilinger, M. A. Horne, and A. K. Ekert. “event-ready-detectors” bell experiment via entanglement swapping. *Phys. Rev. Lett.*, 71(26):4287–4290, Dec 1993.
- [22] Daniel Gottesman and Isaac L. Chuang. Demonstrating the viability of universal quantum computation using teleportation and single-qubit operations. *Nature*, 402(6760):390–393, Nov 1999.



- 
- [23] H.-J. Briegel, W. Dür, J. I. Cirac, and P. Zoller. Quantum repeaters: The role of imperfect local operations in quantum communication. *Phys. Rev. Lett.*, 81(26):5932–5935, Dec 1998.
  - [24] Michael Reck, Anton Zeilinger, Herbert J. Bernstein, and Philip Bertani. Experimental realization of any discrete unitary operator. *Phys. Rev. Lett.*, 73(1):58–61, Jul 1994.
  - [25] Tzu-Chieh Wei, Julio T. Barreiro, and Paul G. Kwiat. Hyperentangled bell-state analysis. *Phys. Rev. A*, 75(6):060305, Jun 2007.
  - [26] Lev Vaidman and Nadav Yoran. Methods for reliable teleportation. *Phys. Rev. A*, 59(1):116–125, Jan 1999.
  - [27] C.P.E. Gaebler. Distinguishability of hyperentangled bell states. *Senior Thesis, Harvey Mudd College*, May 2009.
  - [28] H. Weinfurter. Experimental bell-state analysis. *EPL (Europhysics Letters)*, 25(8):559, 1994.
  - [29] Samuel L. Braunstein and A. Mann. Measurement of the bell operator and quantum teleportation. *Phys. Rev. A*, 51(3):R1727–R1730, Mar 1995.
  - [30] Markus Michler, Klaus Mattle, Harald Weinfurter, and Anton Zeilinger. Interferometric bell-state analysis. *Phys. Rev. A*, 53(3):R1209–R1212, Mar 1996.
  - [31] Paul G. Kwiat and Harald Weinfurter. Embedded bell-state analysis. *Phys. Rev. A*, 58(4):R2623–R2626, Oct 1998.
  - [32] Carsten Schuck, Gerhard Huber, Christian Kurtsiefer, and Harald Weinfurter. Complete deterministic linear optics bell state analysis. *Phys. Rev. Lett.*, 96(19):190501, May 2006.
  - [33] Peter van Loock and Norbert Lütkenhaus. Simple criteria for the implementation of projective measurements with linear optics. *Phys. Rev. A*, 69(1):012302, Jan 2004.
  - [34] Angelo Carollo and G. Massimo Palma. The role of auxiliary photons in state discrimination with linear optical devices. *Journal of Modern Optics*, 49(7):1147–1155, 2002.

- [35] Rupert Ursin, Thomas Jennewein, Markus Aspelmeyer, Rainer Kaltenbaek, Michael Lindenthal, Philip Walther, and Anton Zeilinger. Communications: Quantum teleportation across the danube. *Nature*, 430(7002):849, Oct 2004.
- [36] Julio T. Barreiro, Nathan K. Langford, Nicholas A. Peters, and Paul G. Kwiat. Generation of hyperentangled photon pairs. *Phys. Rev. Lett.*, 95(26):260501, Dec 2005.
- [37] John Calsamiglia. Generalized measurements by linear elements. *Phys. Rev. A*, 65(3):030301, Feb 2002.